Chapter 1

General introduction into membrane transport and a description of the different types of ATP Binding Cassette (ABC) transporters

1.1 Membrane transport

All cells are surrounded by at least one membrane, which keeps the intracellular content separated from the outside. The membrane consists of lipids that form a bilayer (two molecules thick) that is poorly permeable for hydrophilic compounds. Nonetheless, all nutrients that cells use to maintain themselves and/or divide need to be transported across the lipid bilayer. At the same time the cells need to extrude waste products. Whereas some small uncharged molecules can freely diffuse through the lipid bilayer (such as oxygen and nitrogen), most compounds cannot pass the membrane at sufficiently high rates and need to be transported by membrane-embedded proteins. Cellular and environmental conditions dictate the need for widely diverse transport mechanisms, e.g. with respect to rates and affinities for the substrates. Carbon sources that are required in large amounts need

to be transported with a high flux for optimal growth, but they do not require high affinity transport when the extracellular concentrations are high. Glucose has been reported to be transported into *Escherichia coli* cells with $\sim 10^6$ molecules per second (Phillips & Quake, 2006). In contrast, for micronutrients such as vitamins only a small flux is needed, and for substrates of low abundance, high affinity transport is required. High affinity transport can for instance be required to take up metals that can be present in trace amounts only but function as essential co-factors. For essential substrates such as sugars, various transport systems may be present. When these substrates are scarce the cells can use specific transporters that bind the substrates with high affinity and accumulate them against large concentration gradients. The cells use other transporters with lower affinity and higher capacity, when the substrates are highly abundant (Higgins, 1992). These lower affinity transporters achieve larger fluxes over the membrane, so that the cells can grow faster.

For molecules that cannot diffuse across the membrane at sufficiently high rates, transport over the membrane is mediated by proteins. In *Escherichia coli* $\sim$8% of the protein-coding genes are transporters, in *Lactococcus lactis* this number is $\sim$7% (http://www.membranetransport.org/index.html). Transport is so important for cells that they continuously spend $\sim$10-60% of their energy requirement in pumping molecules across cell membranes (Rees et al., 2009).

Even though bacteria can synthesize many of the components they need for growth, it is usually more energy-efficient to take them up from the environment. For example histidine synthesis from PRPP (5-phosphoribosyl-α-1-pyrophosphate) and ATP (adenosine-5'-triphosphate) requires 41 ATP equivalents, while the hydrolysis of only 1-2 ATP molecules is required to transport it into the cell (Ames, 1986; Higgins, 1992). The energy that is saved by using compounds from the environment is probably the reason why prokaryotes have so many different importers.

Transport proteins embedded in the membrane can be divided into different classes (figure 1.1). There are proteins that mediate passive transport via facilitated diffusion. Passive transport does not require input of energy, but can only mediate transport of a molecule down its electrochemical gradient, e.g. from a higher to a lower concentration for uncharged molecules. The transport proteins involved in passive transport are either channels or uniporter carrier proteins. Channels span the lipid bilayer and form a continuous pore that allows (often a certain specific) molecule to pass and are mostly used for inorganic ions or small molecules such as

K^+, Na^+, Ca^{2+}, Cl^-, H^+ or H_2O. Channels allow molecules to cross the membrane via diffusion without need for a large conformational change of the protein (other than required for gating), which makes the transport very rapid. Some channels are conducting transport at rates near the diffusion limit in water. Channels for small substrates often select for a specific substrate based on size and/or charge. Channels that also let large molecule pass are always nonspecific. An example is the mechanosensitive channel of large conductance (MscL). When opened these channels form large holes in the cell membrane, which non-specifically allow the passage of molecules up to 6.5 kDa (Bogaart et al., 2007). These channels also dissipate the necessary gradients of e.g. protons and sodium ions across the membrane as well as the membrane potential. Therefore MscL is used only as an emergency valve when cells would otherwise burst due to an osmotic downshock. Other channels that form large pores, such as antimicrobial peptides, are produced specifically to destroy cells.

Carrier proteins embedded in the lipid bilayer can specifically transport small and large molecules. They bind the molecule on one site of the membrane, undergo a conformational change and release the molecule on the other side of the membrane. The rates of such transport processes are usually not diffusion-limited, but they follow the rate of the conformational change of the protein. Uniporter carrier proteins only facilitate the diffusion of the substrate down its electrochemical gradient.

To be able to accumulate molecules inside the cell or to deplete unwanted molecules from the inside, active transport is needed, which requires input of energy. Either chemical or light energy (in primary active transport) or energy stored in electrochemical gradients of other molecules/ions across the membrane (secondary active transport) can be used. Secondary active transporters can couple the transport of one molecule against its electrochemical gradient to that of another molecule that is transported down its gradient and thereby fuels the transport. The second molecule can be transported in the same direction (symporter) or in an opposite direction (antiporter).

The rest of this thesis describes ATP-driven transporters from the ABC superfamily, which is the largest transporter family known and its members are mostly primary transporters.

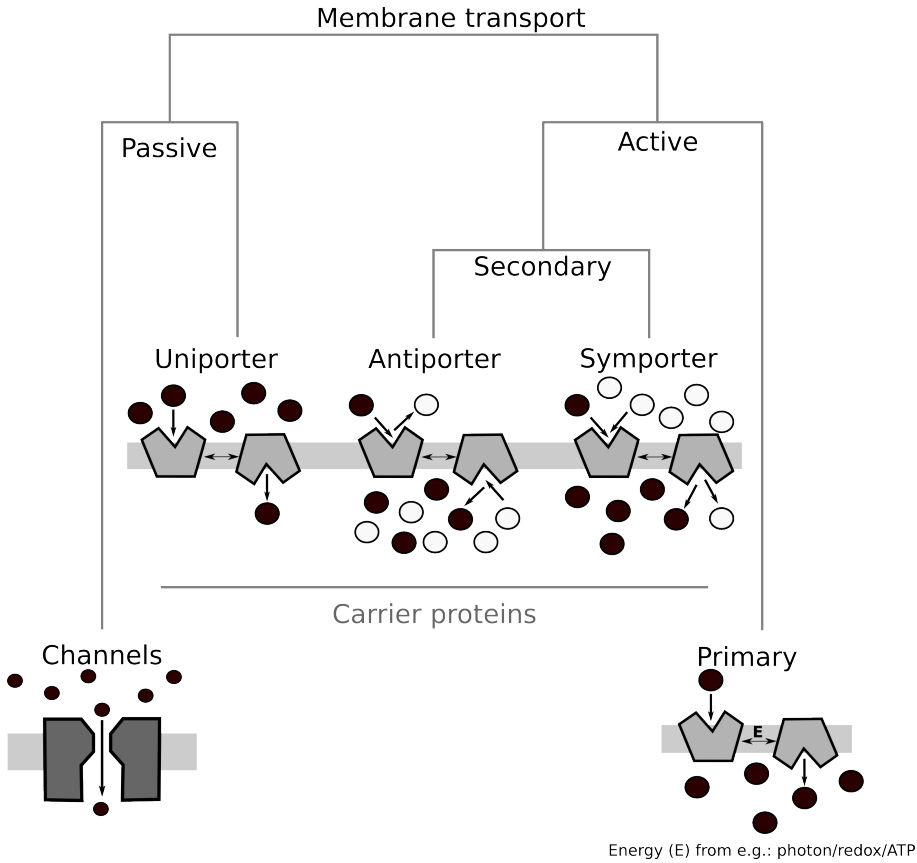

Figure 1.1. **The different classes of transporters are schematically shown.** Passive transporters allow substrates to cross the membrane down their electrochemical gradient, while active transporters can accumulate substrates against the gradient. Channels form a (selective) pore in the membrane. Carrier proteins and primary transporters bind their substrate at one site of the membrane and release it on the other side. Secondary active transporters fuel the transport of a molecule against a gradient by co-transporting a molecule down its electrochemical gradient. This can either be in the same (symporter) or in the opposite (antiporter) direction. Primary transporters use energy from an external source such as light or ATP.

1.2 ABC transporters

The largest group of primary transport systems are ATP-Binding Cassette (ABC) transporters that couple transport of a substrate across the membrane to the hydrolysis of the phosphate bond between the γ- and the β-phosphate of adenosine-5′-triphosphate (ATP). Free energy ($\Delta G'$) is released when ATP is converted into adenosine-5′-diphosphate (ADP) and orthophosphate (P_i). There is a contribution from the ΔG_0 (-30.5 kJ/mol), which reflects the loss of the negative charge density on the three adjacent phosphates that destabilize ATP and the stabilization of

orthophosphate by multiple resonance structures (Berg et al., 2002). In addition there is a contribution of ∼-20 kJ/mol from the concentration term, reflecting the high [ATP]/[ADP] ratio normally maintained in cells (this is $\sim 1 * 10^3$ while at equilibrium this ratio would be $1 * 10^{-7}$ because of the low ΔG_0) (Berg et al., 2002; Nicholls & Ferguson, 2002). Thus, the $\Delta G'$ of ATP hydrolysis is around -50 kJ/mol under physiological conditions (Berg et al., 2002). ABC transporters use this free energy to transport substrates. In exporters substrates are transported to the trans side of the membrane (relative to the nucleotide-binding domains), whereas importers translocate their substrates in the opposite direction. This means that for prokaryotes, exporters transport the substrate to the outside, while importers transport substrates to the inside of the cell. Exporters are found in all kingdoms of life, but importers are found in prokaryotes only. In this thesis the focus will be on prokaryotic transporters. In *Lactococcus lactis* (a Gram-positive bacterium) 34.3 % of the transporters are ABC transporters, in *E. coli* (a Gram-negative bacterium) this number is around 19.5 % (http://www.membranetransport.org/). In the *E. coli* K12 strain there are 50 classified ABC importers and 15 ABC exporters (Moussatova et al., 2008). There has been a lot of interest in ABC transporters not only because it is such a large family, but also because some ABC exporters are involved in drug resistance of bacteria and cancer cells. Another kind of ABC exporter (transporter associated with antigen processing, TAP) is required for antigen loading on major histocompatibility complex (MHC) class I molecules and thus plays an important role in viral inhibition (Parcej & Tampé, 2010). ABC importers may be potential targets for antibiotics, since they exist only in prokaryotes.

For substrate translocation, ABC transporters switch between an outward facing and an inward facing conformation. This cycle must be linked to ATP binding and hydrolysis, ADP and P_i release, and substrate binding and release at opposite sides of the membrane. The structures of several ABC transporters in different conformations have been resolved using X-ray crystallization (table 1.1). These crystal structures have provided much insight in the transport mechanism, but a comprehensive understanding of the transport cycle is still lacking.

Table 1.1. **List of ABC-transporters of which the structure is determined by X-ray crystallography** Sources: http://blanco.biomol.uci.edu/mpstruc/listAll/list and www.pdb.org

Type I importers	Remarks:	Substrate bound:	Resolution (Å):	PDB code(s)
Molybdate transporter $ModB_2C_2$ complexed with ModA: *Archaeoglobus fulgidus*	Complete transporter, inward facing conformation, tungstate bound in SBP (closed conformation)	Mg^{2+}, Phosphate, Tungstate	3.10	2ONK
Crystal structure of *A. fulgidus* periplasmic binding protein ModA with bound molybdate	SBP only, closed state, cluster D SBP	Mg^{2+}, Molybdate	1.60	2ONR
Crystal structure of *A. fulgidus* periplasmic binding protein ModA with bound tungstate	SBP only, closed state, cluster D SBP	Mg^{2+}, Tungstate	1.55	2ONS
$ModB_2C_2$ Molybdate ABC transporter in a trans-inhibited state: *Methanosarcina acetivorans*	Inward facing conformation of the complex, without SBP bound	Mg^{2+}, Tungstate	3.00	3D31
Crystal structure of *M. acetivorans* periplasmic binding protein ModA with molybdate bound	SBP only, closed state, cluster D SBP	Mg^{2+}, Molybdate	2.25	3K6X, 3K6W
Crystal structure of *M. acetivorans* periplasmic binding protein ModA in apo-form	SBP only, open state	-	1.95	3K6U
$MalFGK_2$-MBP Maltose uptake transporter complex: *Escherichia coli*	Outward conformation stabilized by a mutation in the NBDs (MalK E159Q)	Maltose, ATP	2.80	2R6G
$MalFGK_2$ Maltose uptake transporter complex: *Escherichia coli*	TM helix 1 deleted, in inward resting state, without maltose binding protein	-	4.50	3FH6
$MalFGK_2$-MBP Maltose uptake transporter complex: *Escherichia coli* MBP(G69C/S337C)	Pre-translocation intermediate state with mutated MBP (G69C/S337C) that stabilizes the closed substrate bound conformation by a cross-link	Maltose	3.10	3PVO

Continued on next page

	Remarks:	Substrate bound:	Resolution (Å):	PDB code(s)
MalFGK$_2$-MBP Maltose uptake transporter complex: *Escherichia coli*	Outward-facing complex with maltose binding protein	AMP-PNP, Mg^{2+}, Maltose	2.20	3RLF
MalFGK$_2$-MBP Maltose uptake transporter complex: *Escherichia coli*	Outward-facing complex with maltose binding protein	ADP, Mg^{2+}, Maltose, Vanadate	2.40	3PUV
MalFGK$_2$-MBP Maltose uptake transporter complex: *Escherichia coli*	Outward-facing complex with maltose-binding protein	ADP, Mg^{2+}, Maltose, $AlFMg_4$	2.30	3PUW
MalFGK$_2$-MBP Maltose uptake transporter complex: *Escherichia coli*	Outward facing complex with maltose binding protein	ADP-BeF_3, Mg^{2+}, Maltose	2.30	3PUX
MalFGK$_2$-MBP Maltose uptake transporter complex: *Escherichia coli*	Outward-facing complex, after crystal soaking the pre-translocation intermediate state, with MBP	AMP-PNP, Mg^{2+}, Maltose	3.10	3PUY
MalFGK$_2$-MBP Maltose uptake transporter complex: *Escherichia coli*	Pre-translocation intermediate state of the complex, with MBP	AMP-PNP, Mg^{2+}, Maltose	3.10	3PUZ
Structures of the MBP maltose-binding protein in isolation	Various open and closed state structures available, cluster D SBP	Structures with different ligands available	1.67	1ANF, 1DMB, 1EZ9, 1EZO, 1EZP, 1FQA, 1FQB, 1FQC, 1FQD, 1MDP, 1MDQ, 1OMP, 4MBP
MetNI Methionine uptake transporter complex: *Escherichia coli*	Inward-facing conformation	-	3.70	3DHW
MetN-C2 domain	ATP-binding domain only	-	2.10	3DHX

Continued on next page

Type II importers	Remarks:	Substrate bound:	Resolution (Å):	PDB code(s)
$BtuC_2D_2$ Vitamin B_{12} transporter: *E. coli*	Outward facing structure	Cyclo-tetra-meta-vanadate	3.20	1L7V
$BtuC_2D_2$-F Complex; $BtuC_2D_2$ vitamin B_{12} transporter + BtuF binding protein: *E. coli*	Intermediate occluded state. The translocation pore is closed from both sites. BtuF (SBP) is in an open state	-	2.60	2QI9
BtuF structures of substrate binding protein in isolation with or without substrate	SBP only, cluster A SBP. Substrate bound or not bound both in closed state	With or without vitamin B12	2.00	1N2Z, 1N4A, 1N4D
$HI1470_2/1471_2$ Putative metal-chelate-type ABC transporter: *Haemophilus influenzae*, renamed $MolB_2C_2$ since the binding protein (Hi1472 or MolA) was shown to bind tungstate/molybdate	Inward facing complex without SBP	-	2.40	2NQ2
Hi1472 or MolA, substrate binding protein of the $Hi1470_2/1471_2$ importer	Shows that Hi1472 is not a metal chelate binding protein, but binds molybdate/tungstate	Molybdate Tungstate	1.50 1.70	3PSH 3PSA

ECF-type importers	Remarks:	Substrate bound:	Resolution (Å):	PDB code(s)
-	**Currently no complete transporter is crystallized**			
S-component for riboflavin, RibU of *Staphylococcus aureus*	S-component substrate bound	Riboflavin	3.60	3P5N
S-component for thiamin, ThiT of *Lactococcus lactis*	S-component substrate bound	Thiamin	2.00	3RLB
S-component for biotin, BioY of *Lactococcus lactis*	S-component substrate bound (presented in chapter 4)	Biotin	2.10	4DVE
EcfA (NBD) of *Thermotoga maritima* (TM_0222)	ATP-binding domain only	-	2.30	2YZ2
EcfA (NBD) of *Sulfolobus tokodaii* (ST1066)	ATP-binding domain only	-	1.90	2PJZ
EcfA (NBD) of *Clostridium perfringens* ($CbiO_1$)	ATP-binding domain only	-	2.30	3GFO

Continued on next page

Exporters	Remarks:	Substrate bound:	Resolution (Å):	PDB code(s)
Sav1866 Multidrug transporter: *Staphylococcus aureus*	Outward-facing	ADP	3.00	2HYD
Sav1866 Multidrug transporter: *Staphylococcus aureus*	Outward-facing	AMP-PNP	3.40	2ONJ
MsbA Lipid "flippase" with bound ANP-PNP: *Salmonella typhimurium*	Outward-facing with nucleotide bound	ANP-PNP	3.70	3B6O
MsbA Lipid "flippase" with bound ANP-PNP: *Salmonella typhimurium*	Outward-facing with nucleotide bound	ANP-PNP	4.50	3B5Y
MsbA Lipid "flippase" with bound ADP, vanadate: *Salmonella typhimurium*	Outward-facing with nucleotide bound	ADP, Vanadate	4.20	3B5Z
MsbA Lipid "flippase": *E. coli*	Inward-facing, open apo structure	-	5.30	3B5W
MsbA Lipid "flippase" with bound AMP-PNP: *Vibrio cholerae*	Inward-facing, closed apo structure	-	5.50	3B5X
P-Glycoprotein: *Mus musculus* (mouse)	Inward-facing	-	3.80	3G5U
P-Glycoprotein: *Mus musculus* (mouse)	Inward-facing	QZ59-RRR	4.40	3G60
P-Glycoprotein: *Mus musculus* (mouse)	Inward-facing	QZ59-SSS	4.35	3G61

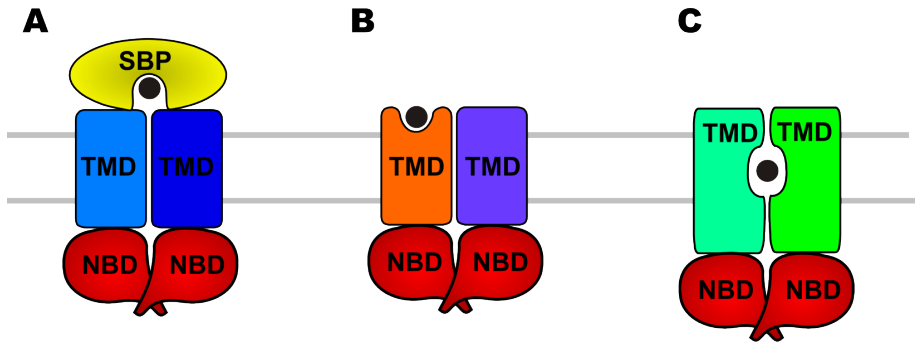

Figure 1.2. **Schematic representation of the various types of ABC-transporters.** The places where the substrate is initially bound are indicated with an indentation and a black circle that indicates the substrate. All ABC transporters consist of two transmembrane domains (TMDs) and two nucleotide-binding domains (NBDs). The NBDs are the hallmark of the ABC transporters. The fold of the NBDs is conserved and they also have conserved sequence motifs. ABC transporters can be importers (A and B) or exporters (C). Importers are divided into importers with a soluble substrate binding protein/domain (SBP-dependent, A) and without this additional domain (the ECF-type, B). The importers that are dependent on a soluble substrate-binding domain are further divided in two types depending on the fold of their TMDs: type I and type II. In type I and II ABC importers (A) the substrate is initially bound by the SBP and then delivered to the TMDs. The SBP can be a periplasmic protein (Gram-negative bacteria), it can have a lipid anchor or it can be a domain linked to the TMD. For the type I maltose transporter $MalFGK_2$ there is also a binding site in one of the two TMDs. In the ECF-type or type III importer (B), one of the TMDs is specialized to bind the substrate with high affinity. In exporters (C) the substrate-binding site is found in between the TMDs.

ABC transporters always consist of two transmembrane domains (TMDs) and two nucleotide-binding domains (NBDs) (figure 1.2). The nucleotide-binding domains are conserved among all ABC transporters, but the transmembrane domains differ between the different types of transporters. ABC transporters are divided into importers and exporters according to the direction of the transport. Importers are further divided into three types, numbered by the time of their discovery. Type I and type II importers contain an additional soluble substrate binding domain (SBP) while type III or ECF-type (ECF stands for Energy Coupling Factor) importers do not (figure 1.2). Type I and II importers are divided based on the fold of their TMDs. Up to date only one type/fold of ABC exporter has been described. The recent discovery of ECF-type transporters will be elaborated on in chapter 2 and structural and functional studies will be presented in chapters 3-6.

Type I and II ABC importers are abundantly present in prokaryotes. ECF-type ABC are most widespread (but not exclusively) among Gram-positives. ABC exporters are found in all kingdoms of life. Prokaryotic ABC transporters are usually assembled from different protein subunits, while eukaryotic exporters are generally composed of one polypeptide chain or a dimer of two polypeptides.

These eukaryotic polypeptides contain multiple domains. In all crystallized exporters the nucleotide-binding domain is fused to the transmembrane domain. The bacterial exporters $MsbA_2$, $Sav1866_2$ and TM287/TM288 are dimers of two polypeptide chains. Each chain contains one TMD and one NBD. The eukaryotic exporter PgP consists of one polypeptide chain that contains two NBDs and two TMDs.

ABC transporters are used to transport a large variety of substrates, ranging from inorganic ions to macromolecules such as polypeptides. Previously a difference was reported in the substrate preferences of the various importers. Type I ABC importers have been reported to mediate the uptake of ions, sugars and amino acids. Currently it is known that they can transport many other substrates. Many ECF-type transporters transport vitamins and transition metal ions, but they are also predicted to transport (precursors of) amino acids and nucleosides (table 1.2). Type II ABC importers ($BtuC_2D_2$ and $Hi1470_2/1471_2$) have been reported to only transport large metal chelates into the cell, such as heme and cobalamine (vitamin B_{12}). Recently, however, crystal structures of the substrate-binding protein Hi1472 (renamed as MolA) became available with tungstate or molybdate bound (Tirado-Lee et al., 2011). Hi1472 is the substrate-binding protein of the crystallized type II importer $Hi1470_2/1471_2$ (renamed $MolB_2C_2$). This transporter was predicted to transport a metal chelate into the cell. However its binding protein, Hi1472, was shown to bind tungstate and molybdate instead of metal chelates (Tirado-Lee et al., 2011). Tungstate and molybdate are also substrates of type I transporters. Other examples of substrates that can be transported by various kinds of ABC importers are cobalamine which can be imported by type II and ECF-type transporters and thiamin which is transported by ECF-type and type I importers. The difference between the various importers apparently does not (only) relate to the substrate specificity (George & Jones, 2011).

ABC exporters are known to be involved in the transport of proteins (e.g. toxins, hydrolytic enzymes, S-layer proteins, lantibiotics, bacteriocins, and competence factors), lipids, fatty acids, cholesterol and drugs. Most drug exporters transport a large variety of drugs out of the cell and are therefore called multi-drug resistant (MDR) transporters.

Table 1.2. **Substrates of ECF-type ABC importers** (see also chapter 2)

S-component	Substrate	Substrate
BioY	Biotin	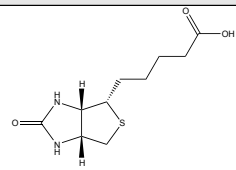
NikMN	Nickel ion	Ni^{2+}
CbiMN	Cobalt ion	Co^{2+}
YkoE	Thiamin precursor	(see ThiT for thiamin)
MtsT	Methionine precursor	Methionine: 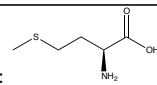
HtsT	not known	
QrtT	Queuosine precursor	Queuosine: 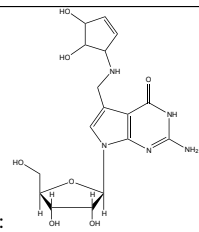
CbrT	Cobalamin precursor	Cobalamin: 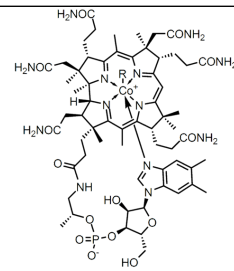 R = 5'-deoxyadenosyl, Me, OH, CN
MtaT	Methylthioadenosine	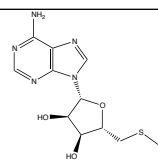
RibU	Riboflavin	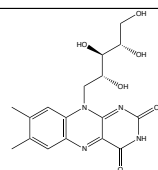

Continued on next page

S-component	Substrate	Substrate
FolT	Folate	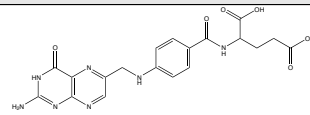
QueT	Queuosine precursor	(see QrtT for Queuosine)
PanT	Pantothenate	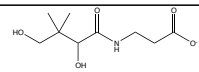
ThiT	Thiamin	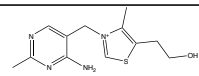
ThiW	Thiazole	
NiaX	Niacin	
TrpP	Tryptophan	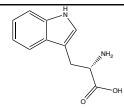
PdxU	Pyridoxine	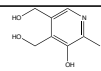
PdxU2	Pyridoxine related	(see PdxU for pyridoxine)
CblT	Cobalamin precursor	(See CbrT for cobalamin)
LipT	Lipoate	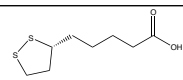

1.3 Nucleotide-binding domain (NBD)

All ABC transporters contain two nucleotide-binding domains (NBDs), also called ATPases or ATP-binding cassettes (ABCs) that bind and hydrolyse ATP. Each NBD contains around 200 amino acids and two subdomains: the larger RecA-like domain (which resembles the RecA protein that is not functionally related) and the structurally more diverse α-helical domain (figure 1.3 and 1.4).

Although NBDs can vary in sequence they share the same fold (figure 1.4) and they can be identified at the sequence level by a specific set of highly conserved motifs (figure 1.3 and 1.5). The motifs in the RecA-like subdomain are mentioned first. The A-loop contains a conserved aromatic residue (usually a tyrosine) that helps to position the ATP by stacking with the adenine ring (figure 1.3). The P-loop or Walker A motif (GXXGXGK(S/T)) is a glycine-rich phosphate-binding loop that contains the highly conserved lysine residue. Backbone amide nitrogens and

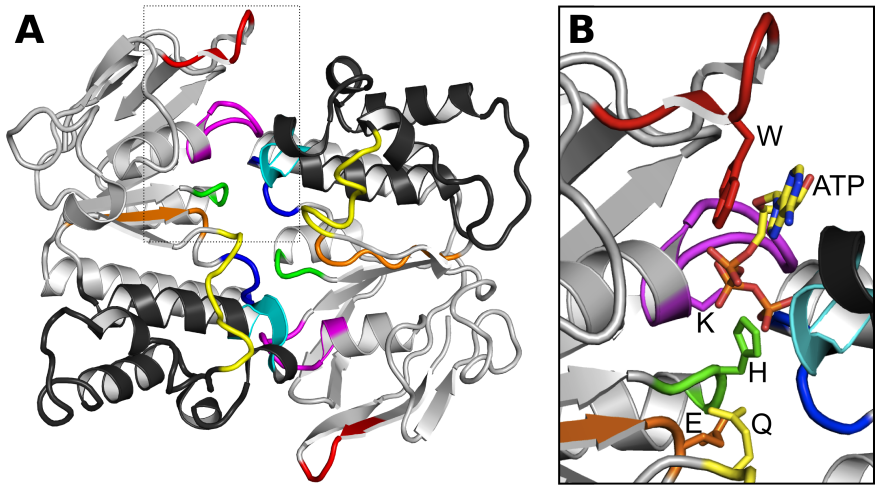

Figure 1.3. **The dimer of the nucleotide binding domains $MalK_2$ with ATP bound (PDB: 1Q12).** The α-helical domains are colored in black and the RecA-like domains are colored in grey. The additional regulatory C-terminal domain that is present in MalK is not shown for clarity. The conserved sequences that are discussed in the text are indicated in both monomers. The A-loop is shown in red. The Walker A is shown in magenta, the Walker B in orange, the SALD-loop in blue and the ABC motif of the α-helical domain in cyan. The H-loop is in green and the Q-loop is indicated in yellow. The panel indicated in A is shown again in B; this is a zoom in on one of the ATP-binding sites. The ATP molecule is shown in stick-model with the carbon in yellow, nitrogen in blue, oxygen in red and phophorus in tan. The hydrophobic residue of the A-loop is shown in red sticks (in MalK this is a tryptophan [W]). The conserved lysine (K) of the Walker A is shown in magenta sticks. The histidine (H) of the H-loop is shown with green sticks. The conserved glutamate (Q) of the Q-loop is in yellow stick representation and the glutamate (E) at the end of the Walker B motif is shown in orange stick representation.

especially the ε-amino group of the lysine form extensive hydrogen bonds with the β- and the γ-phosphate of ATP. The aspartate residue (D) of the Walker B motif ($\phi\phi\phi\phi$DE, in which ϕ is a hydrophobic amino acid) coordinates the magnesium ion, via coulomb interactions (the catalytic Mg^{2+} and the aspartate are 3.8 Å apart [PDB = 3PUZ], the Mg^{2+} is not shown in figure 1.3). An acidic residue at the end of the Walker B motif (often a glutamate, E) has been proposed to be the general base that polarizes the attacking water molecule, although this is still under debate (for an overview see (Davidson et al., 2008)). The Walker B is followed directly by the D-loop (SALD). The D-loops from opposing monomers run alongside each other in the dimer. Changes in the conformation of the D-loop affect key residues in the catalytic sites, thereby forming or breaking the ATP hydrolysis site during the catalytic cycle. The H-loop (or switch region, that contains a highly conserved

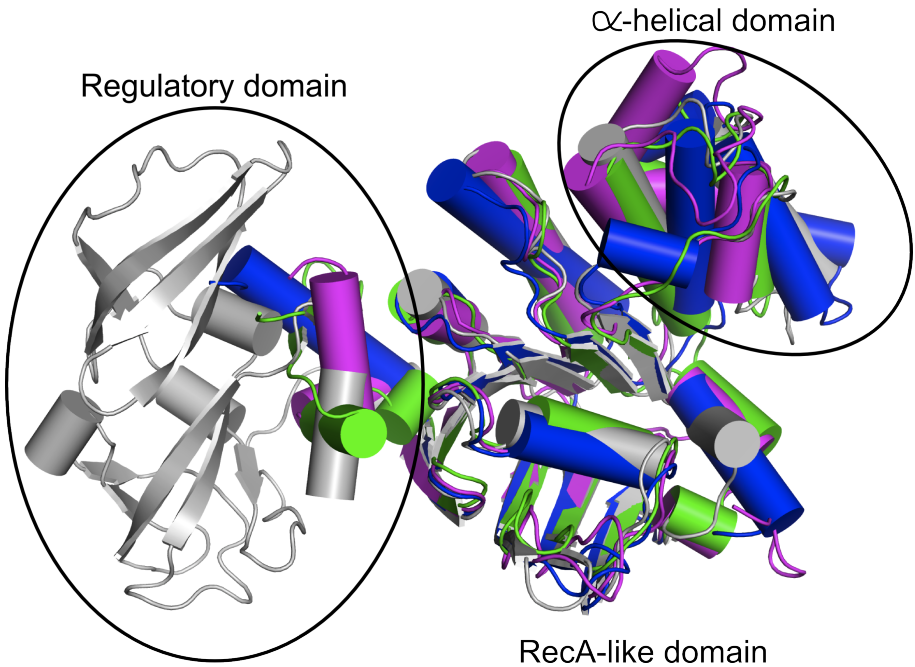

Figure 1.4. **Cartoon representation of the nucleotide-binding domain of a type I importer (MalK, PDB: 1Q1B, in grey), a type II transporter (BtuD PDB: 2QI9, in green), an ECF-type importer (EcfA from *Clostridium perfringens* PDB: 3GFO, in blue) and an exporter (SAV1866 PDB: 2HYD, in magenta).** One NBD monomer is shown for each transporter and they were structurally aligned in pymol. It can be seen that the NBDs from all the different transporter types share the same fold. It can also be seen that the RecA-like domain is more structurally conserved than the α-helical domains. The only parts that do not align are the additional C-terminal helices or domains, that are present in many of the NBDs but that are not directly involved in ATP hydrolysis. They have a regulatory function.

histidine) forms a hinge between a β-strand and an α-helix near the C-terminal of the NBD. The histidine interacts with the conserved aspartate from the D-loop, the proposed general base (often a glutamate) at the end of the Walker B motif and the γ-phosphate of the ATP (Oldham & Chen, 2011b). It is proposed to be involved with the positioning of the attacking water, the general base and the magnesium ion (Oldham & Chen, 2011b; Zaitseva et al., 2005). Also in the RecA-like subdomain, at the interface with the α-helical subdomain, is the Q-loop. This loop of $\sim$8 residues with a conserved glutamine at its N-terminus, links the RecA-like domain to the α-subdomain and forms an important part of the interface of the NBDs with the TMDs. Conformational changes in the Q-loop switch the glutamine in and out of the active site during the hydrolysis cycle, forming the active site when MgATP is bound and disrupting it once ATP is hydrolyzed. The ABC signature motif (or C-motif, LSGGQ) is found in the α-helical subdomain and is the characteristic feature

of the ABC superfamily (figure 1.3 and 1.5). This LSGGQ-motif is at the N-terminal end of a long helix that directs the positive charge of the helical dipole towards the γ-phosphate of ATP.

NBDs form homo- or hetero-dimers in a head-to-tail fashion with the ABC signature motif of one of the domains close to the Walker A and B motif of the other domain (figure 1.3 and 1.5). ATP hydrolysis takes place at the interface between the two monomers. When ATP is bound, the NBDs come close together to promote ATP hydrolysis. Subsequent ATP hydrolysis and/or the release of ADP and P_i destabilize the dimer and the NBDs go further apart again. During this cycle the RecA-like subdomain and the α-helical subdomain within both NBDs also rotate towards each other when ATP is bound and away from each other after hydrolysis and/or ADP and P_i release. These conformational changes transform the chemical energy of ATP hydrolysis into conformational energy that can be transmitted to the TMD and used for transport.

Most NBD dimers have two ATP hydrolysis sites and are expected to use the hydrolysis of one or two ATP molecules for a complete transport cycle. The osmoregulatory ABC transporter from *Lactococcus lactis*, OpuA, was found to hydrolyze 2 ATPs per translocated substrate (Patzlaff et al., 2003). For OpuA the stoichiometry could be accurately determined because of strict coupling between ATPase hydrolysis and transport, while for many other transporters high background ATPase activity in the absence of substrate preclude accurate measurements. This futile hydrolysis of ATP may be a natural property of some transporters, although the use is not clear since energy is spent in absence of transport. The measured ATPase activity in the absence of transport might also be due to artificial experimental conditions. In the NBDs of some ABC transporters one of the two sites is degenerate and cannot hydrolyse ATP because of mutation(s). Probably these transporters only require the hydrolysis of one ATP per transport cycle. In some ABC-transporters with two intact hydrolysis sites one site can be inactivated by mutation without loss of function (shown for the histidine transporter (Nikaido & Ames, 1999)), while in others this is not the case (as shown for the maltose transporter (Davidson & Sharma, 1997)). In both the histidine and the maltose transporter positive cooperation between the two ATP hydrolysis sites is observed. An explanation for this observation could be that two ATP molecules have to bind so that both sides are occupied, before the ATP domains can close (Davidson et al., 2008). But whether subsequently both ATP molecules or just one of the two is hydrolyzed per translocation cycle remains unclear.

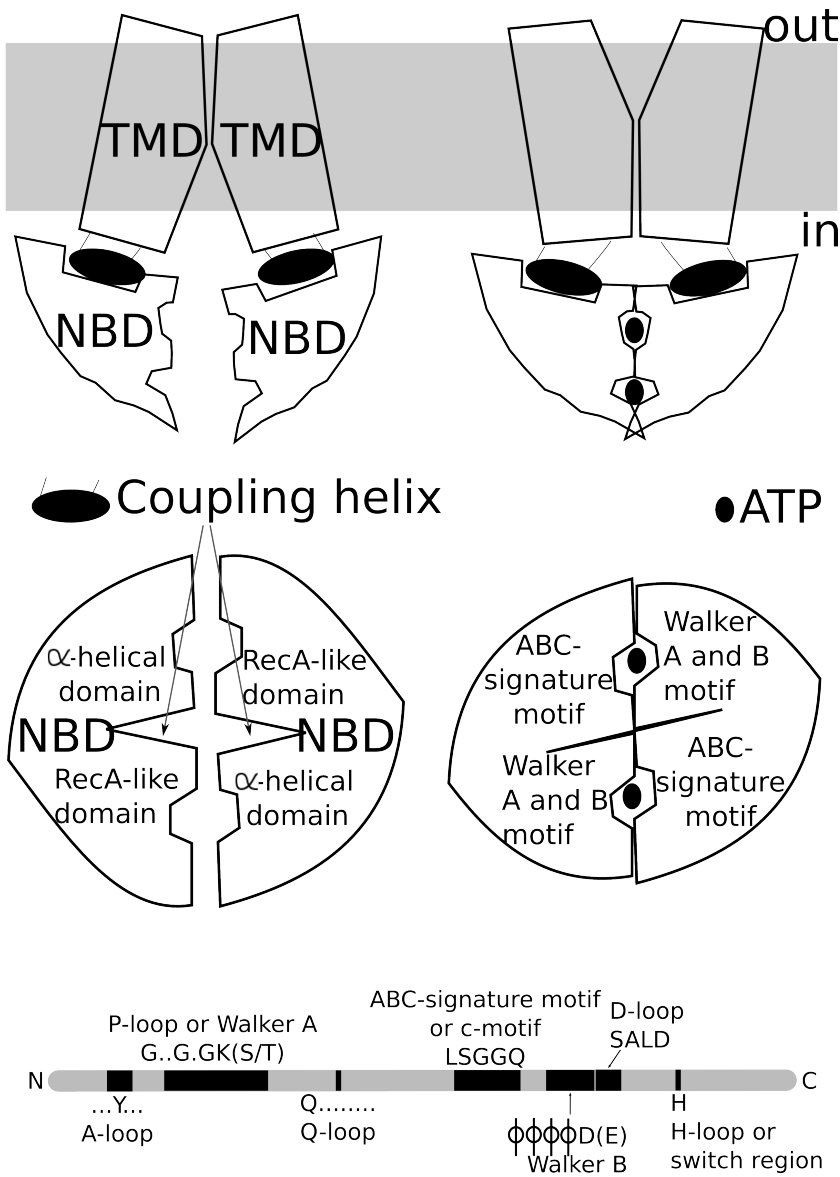

Figure 1.5. **Translocation cycle of an ABC transporter driven by ATP hydrolysis in the nucleotide binding domains (NBDs)** schematically shown on top. Conformational changes upon ATP hydrolysis in the nucleotide-binding domains (NBDs) are linked to conformational changes in the TMDs via so-called coupling helices. Middle panel: the NBDs in more detail, showing the two domains, the location of the interaction site with the coupling helices from the TMDs (indicated by the arrows) and the sites of ATP binding and hydrolysis. The left and the right image schematically show the conformational changes in the NBDs upon ATP binding. The lower pannel shows an overview of the sequence of a single NBD with the conserved motifs. Figure adapted from (Locher, 2009; Rees et al., 2009).

1.4 Transmembrane domain (TMD)

Besides the presence of two NBDs, ABC transporters also always have two transmembrane domains (TMDs, figure 1.2). These two TMDs form one translocation pore at their interface, which must be accessible alternately from the inside and from the outside of the membrane to selectively transport the substrate (figure 1.1 and 1.5). However, there are exceptions where the ABC transporter is a channel (e.g. CFTR (Gadsby et al., 2006)), or does not translocate at all (e.g. SUR proteins, complete ABC transporter mimics that regulate K_{ATP} channels (Bryan et al., 2007)). Whereas the NBDs of all ABC transporters are structurally highly similar and all contain various conserved motifs, the TMDs of ABC transporters vary widely in length, sequence and structure (e.g. the structures of type I and II importers and exporters are unrelated). This is probably because they have to accommodate chemically very different molecules during transport. The TMDs of a single transporter can be (nearly) identical (often the two TMDs are homodimers) or considerably different (the two TMDs of the maltose transporter $MalFGK_2$ share only 13% sequence identity). Although the TMDs of type I importers often contain two sets of six TM helices, the number of helices per TMD can vary. Known type II importers have ten TM helices (Jones et al., 2009). Based on the available X-ray crystal structures (table 1.1) three different folds of TMDs are currently known for ABC importers and only one for exporters. However, more folds may exist. The main fold of the TMDs for the various types of transporters will now be discussed.

The two TMDs of type I importers have a core topology of five helices per TMD. In most cases an additional N-terminal helix is present that wraps around the helices of the other TMD and intertwines the TMDs, making a total of twelve TM helices. However, some TMDs contain up to 8 TM helices. The transmembrane helixes of both transmembrane domains are curved and line a relatively wide pore.

Type II ABC importers have two TMDs with each ten TM helices. In the type II fold the TMDs are lined up next to each other; they do not have helices that cross over to the other TMD. In each TMD there is a pseudo two-fold symmetry between the segments containing TM helices 2-5 and TM helices 7-10. These two subdomains have a similar helical packing but with opposite orientation with respect to the membrane. The packing of the helices places TM helix 2 in the centre, where it is in contact with most other helices of the domain. The helices of a single TMD are tightly packed together, and the two TMDs line a narrow pore.

In ECF-type ABC importers one transmembrane domain is formed by EcfT which is homologous for all identified ECF-type transporters and is predicted to have 4-8 TM helices (Eitinger et al., 2010). No structural information about the EcfT is currently available. The second TMD is formed by a so-called S-component. S-components are substrate-binding proteins that are not soluble (in contrast to the SBPs seen in type I and II importers) but hydrophobic integral membrane proteins. They bind the substrate with high affinity and are predicted to contain 4-7 TM helices (chapter 3 and (D. Rodionov et al., 2009)). Structures are now available of three S-components (from different families), which all have a similar fold with 6 tightly packed TM helices (chapter 4 and (Zhang et al., 2010; Erkens et al., 2011)). This fold differs from the TMDs of the other transporters.

All crystal structures of ABC exporters (MsbA, PgP, Sav1866, TM287/TM288) show a common structural fold consisting of a core of two times six TM helices that extends well into the cytoplasm (Dawson & Locher, 2006; Ward et al., 2007; Aller et al., 2009; Hohl et al., 2012). Because of these long helices, the NBDs are 25 Å away from the membrane, which is not the case in any of the crystallized importers. In all crystallized ABC exporters the NBDs are fused to the TM domains. The helices of the TM domains are twisted around each other. Two helices of each TMD cross over to the other TMD. For the lipid flippase MsbA, an inward- and an outward-facing structure is available. In the inward-state one TM domain is formed by TM helices 1, 2, 3, 6, of one and helices 4 and 5 from the other TMD. While in the outward-facing state TM helices 1 and 2 of one subunit and helices 3-6 from the other subunit form one TM domain (Ward et al., 2007).

1.5 Coupling helix

In the structures of ABC exporters and type I and II importers, so called coupling helices are present. A coupling helix is a short α-helix in one of the cytoplasmic loops of the TMD that falls into a groove in the NBD. In this way each NBD is connected to a TMD and the conformational changes in the NBDs caused by ATP binding, hydrolysis and ADP+P_i release can be transduced to a conformational change in the TMDs, resulting in a shift from an outward to an inward conformation or *vice versa* (figure 1.5). The importance of this region of the protein was already recognized before crystal structures were available, as a subset of the coupling helices contain a conserved sequence known as the EAA motif (Mourez

et al., 1997; Oldham et al., 2007; Locher, 2009). Coupling helices are found between transmembrane (TM) helix 3 and 4 of type I importers and between TM helix 6 and 7 of type II importers. In ABC exporters the coupling helix region is found in the intracellular loop (ICL) 2 between TM helix 4 and 5. In exporters where the TMDs are fused to the NBDs, the coupling helix of one TMD interacts with the NBD that is linked to the other subunit. Although the arrangements are different in the different types of transporters, the coupling helices are structurally equivalent (Rees et al., 2009). It is not yet clear if coupling helices are present in ECF-type ABC importers and, if so, where they are located. We have speculated that both coupling helices may come from one of the TMDs, the EcfT, since the S-components (which forms the other TMD) do not have cytoplasmic helices that could function as coupling helices (see below, chapter 4 and (Erkens et al., 2011; Neubauer et al., 2011)).

The region of the NBDs that interacts with the coupling helix of the TMDs contains the Q-loop, which is located in the RecA-like domain at the interface with the α-helical domain. The Q-loop contains a conserved glutamine (Q) that is involved in nucleotide binding (figure 1.3), but structurally varies considerably between NBDs. Changes in this area have been proposed to be connected to coupling of ATP hydrolysis to the transport cycle (Jones & George, 2002). The cleft for the coupling helices in the NBDs is located exactly at the interface between the α-helical subdomain and the RecA-like subdomain, which rotate towards each other in response to ATP binding for ATP hydrolysis.

In the type I maltose importer ($MalFGK_2$) the coupling helices are not the only site of interaction between the TMDs and the NBDs, because the C-terminal segment of one of the TMDs (MalG) is partly inserted between the two NBDs and seems to further order the Q-loop region. Additional interactions are also seen in type II importers, e.g. $BtuC_2D_2$ has an additional helix next to the coupling helix that also interacts with the NBDs. All crystallized exporters contain an additional cytoplasmic coupling helix. This helix is located between TM helix 2 and 3 (ICL1) and interacts directly with the NBD regions that bind the nucleotide adenine ring. Thereby they shield the nucleotide and the active site of the NBDs from the bulk solvent in the ATP-bound closed state. The NBDs of exporters contain an additional motif (the x-loop: TEVGERG) that interacts with both coupling helices (ICL1 and ICL2) of the TMDs. This motif is located just in front of the ABC signature motif. Based on this x-loop motif it was suggested that the coupling mechanism of ATP hydrolysis and transport would go via a distinct mechanism in exporters (Dawson & Locher, 2006).

In intact ABC importers and exporters vanadate traps the NBDs in an occluded state, which does not occur in isolated NBDs. In exporters this dependency on interaction with the TMDs can be explained by the additional cytoplasmic helix that occludes the nucleotide (crystal structure of MsbA with ADP and vanadate PDB: 3B5Z) (Jones et al., 2009). There is also a crystal structure of the type I maltose importer (PDB: 3PVU) with ADP and ortho-vanadate.

1.6 Substrate binding

1.6.1 Type I and II ABC importers

Type I and II ABC importers depend on an additional substrate-binding domain or protein (SBD or SBP, here always called SBP for clarity), besides the four core domains/subunits (2 NBDs and 2 TMDs) described above (figure 1.2). The SBP is a soluble domain or protein that is located on the the other side of the membrane than the cytosolic NBDs. SBPs have a high affinity for their substrate with dissociation constants often in the range of 0.01 to 1 μM (Davidson et al., 2008). Sometimes the dissociation constants are much lower e.g. OpuBC from *Bacillus subtilis* has an affinity of 30 μM for choline (Pittelkow et al., 2011), MolA from *Haemophilus influenzae* has an affinity of $\sim$100 μM for molybdate and tungstate (Tirado-Lee et al., 2011)) or much higher e.g. TbpA from *E. coli* has an affinity of 2.3 nM for thiamin (Soriano et al., 2008) and NR1 from *R. novegicus* has an affinity of 4 nM for glycine (Miyazaki et al., 1999; Ivanovic et al., 1998)). SBPs are either linked in a single polypeptide with the TMD of the transporter, connected to the membrane via a lipid anchor (in Gram-positive bacteria and archaea) or freely diffuse in the periplasm (in Gram-negative bacteria). Even though SBPs vary considerably in sequence and size, and bind numerous chemically unrelated substrates, they have an overall structure that is highly conserved. SBPs have two domains or lobes that are connected via a hinge region (figure 1.6). Based on their structure they can be categorized into six different clusters (table 1.3) (Berntsson et al., 2010).

These clusters differ either by the presence/absence of an additional domain (present in cluster C) or in structure of the hinge region between the two domains. In cluster A this hinge is formed by a rigid helix. In cluster B there are three interconnecting segments between the domains. In cluster D there are two relatively short hinges.

Table 1.3. **Clusters of soluble substrate binding proteins (SBPs)** (Berntsson et al., 2010)

Cluster	Sub-cluster	Types of ligands	Main feature
A	I II	Metal ions Siderophores	Single rigid α-helix connects the two domains
B	-	Carbohydrates, Leu, Ile, Val, autoinducer-2	Three interconnecting segments between the two domains
C	-	Di- & oligopeptides, Arg, cellubiose, nickel	An additional domain. These SBPs are significantly larger
D	I II III	Carbohydrates Putrescine, thiamine Tetrahedral oxyanions	Two relative short hinges between the two domains
E	-	Sialic acid, 2-keto acids, ectoine, pyroglutamic acid	Large flexible helix in between the two domains. Only associated with TRAP transporters.
F	I II III IV	Trigonal planar anions, unknown ligands Methionine Compatible solutes Amino acids	Two hinges in between the two domains as in cluster D, but these hinges are almost twice as long, giving the SBP more flexibility

In cluster E (not found in ABC transporters, only in Tripartite ATP-independent periplasmic (TRAP) transporters) a large helix forms the hinge between the two domains. Cluster F has two hinges between the two lobes like cluster D but these hinges are almost twice as long (Berntsson et al., 2010).

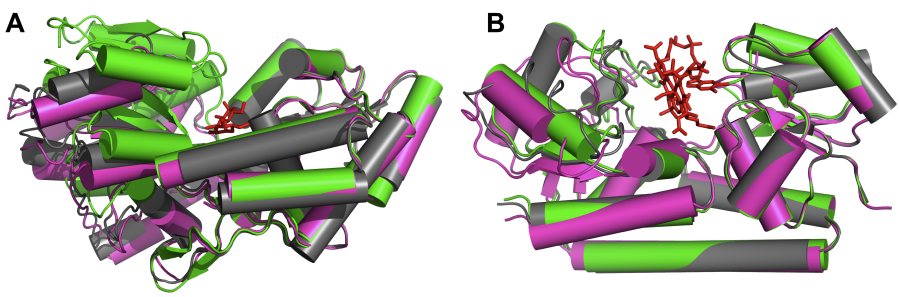

Figure 1.6. **Open and closed conformations of two classes of substrate binding proteins (SBPs).** **A** Cartoon representation of the maltose-binding protein (MBP, a SBP of cluster D) of the type I maltose transporter in a closed conformation with maltose bound (green, PDB: 1ANF), in an open conformation (grey, PDB: 1EZ9), and in the open conformation that is found when it is bound to $MalFGK_2$ (magenta, PDB: 2R6G, only MBP shown). Maltose is indicated with a line representation in red. **B** Cartoon representation of BtuF (a SBP of cluster A) of the type II vitamin B_{12} transporter with ligand bound (green, PDB: 1N4A) and without ligand bound (grey PDB: 1N4D) showed almost the same conformation when crystallized in isolation, but when the whole transporter (the $BtuC_2D_2F$ complex, PDB: 2QI9) was crystallized a slightly more open conformation was found for the SBP (shown in magenta). The ligand, cobalamine, is shown as a line representation in red. **A,B** All SBPs are aligned on one of the two lobes (shown on the right).

Without ligand the two domains of the NBD exist largely in an open conformation, but when substrate is bound the closed conformation is stabilized and the ligand gets trapped in between the two lobes (the Venus fly-trap model, figure 1.6). SBPs bind the substrate at the outside of the cell and when they have bound their substrate, they deliver it to the transporter complex. SBPs have been shown to interact with both TMDs, with one of the two lobes interacting mostly with one of the two TMDs and the other lobe interacting mostly with the other TMD (Higgins, 1992; Hollenstein et al., 2007; Oldham et al., 2007; Hvorup et al., 2007; Pinkett et al., 2007).

Some of the type I and II ABC importers can handle various substrates. This is either because their SBPs can recognize various substrates (e.g. the SBP of the multi-sugar transporter Msm of *Streptococcus mutans* can recognize melibiose, sucrose, raffinose, isomaltotriose, and isomaltotetraose (Tao et al., 1993)), or because the transporter can interact with various SBPs. Examples of the latter are the histidine/lysine/arginine transport system in *Enterobacteriaceae* (a large family of Gram-negative bacteria) which interacts with an SBP for histidine as well as a different SBP for lysine and arginine (Higgins & Ames, 1981), the peptide transporter OppBCDF from *Enterococcus faecalis*, which can not only interact with OppA, which can bind many different peptides, but also with PrgZ which binds one specific peptide (a pheromone) (Leonard et al., 1996), and the oligopeptide/muramyl peptide transport system of *E. coli* where not only the SBP for oligopeptides delivers substrate, but a second SBP can deliver a murein tripeptide (Park et al., 1998). However, the interaction of different SBPs with the same translocator is relatively rare.

In the type I maltose transporter $MalFGK_2$, one of the TMDs (MalF) contains a second binding site for maltose (besides the binding site in the SBP). This binding site is located at the center of the bilayer. It is likely that substrate is moved from the SBP to the central membrane embedded site during the translocations cycle. Up to date this is the only crystal structure where an additional binding site has been found, but it seems likely that it is a more general feature (of type I) importers. In the histidine transporter ($HisMQP_2$-HisJ/LAO) (Speiser & Ames, 1991) mutations in the NBDs ($HisP_2$) lead to transport of histidine in the absence of the SBP (HisJ/LAO). No crystal structure of the histidine transporter is available but its TMDs (HisM and HisQ) are predicted to have 5 TM helices. Therefore it probably is a type I transporter. For the maltose transporter mutants are available in which low-affinity transport of maltose occurs independent of the SBP (Shuman, 1982; Treptow & Shuman, 1985; Davidson et al., 1992).

In the type II $BtuC_2D_2(F)$ structures no substrate was bound in the translocation pathway between the TMDs and no site could be found that resembles a binding pocket. It has been hypothesized that the translocation pathways of the type II ABC importers are inert, teflon-like, with little or no affinity for the substrates (Locher, 2009). This would mean that the specificity of these transporters is entirely dependent on the SBP and its affinity for the TMDs.

1.6.2 Type III or ECF-type ABC importers

In the ECF-type ABC importers (also called ECF transporters) one of the TM domains binds the substrate. These importers therefore do not require an additional SBP. The TMD that binds the substrate is called S-component. S-components have a very high affinity for their substrate, with dissociation constants (K_d) in the low- or subnanomolar range (chapter 4 and (Duurkens et al., 2007; Erkens & Slotboom, 2010; Eudes et al., 2008)). The structures of three S-components have been elucidated. These are RibU, the S-component for riboflavin from *Staphylococcus aureus* (Zhang et al., 2010), as well as two structures from *Lactococcus lactis*: ThiT (the S-component for thiamin) (Erkens et al., 2011) and BioY (the S-component for biotin, chapter 4). All the three proteins were crystallized with their substrate bound (figure 1.7). The substrates are bound near the extracellular face of the protein, although access to the binding site is closed off so that the substrate is occluded. In the high-resolution structures of ThiT and BioY the respective substrates thiamine and biotin are kept in place via an extensive network of hydrogen bonds, ionic interactions and aromatic stackings, explaining the high substrate affinities of these proteins. All three proteins have six transmembrane helices, including a long tilted helix (helix 6) and a very short helix (helix 2) that is preceded by a long loop between helices 1 and 2 (L1), which is partially embedded in the membrane. The C-terminal halves of the proteins (helices 4-6) make most interaction with the substrates, but in all three proteins the L1 loop also contributes to substrate binding. Possibly, this L1 loop is open in the apo-structure and closes upon substrate binding (Zhang et al., 2010; Erkens et al., 2011).

In many ECF transporters one ECF module, consisting of two NBDs ($EcfA_2$ or EcfAA') and a TMD (EcfT), can interact with various S-components (chapter 2). The ECF module from *L. lactis* for instance has been shown to interact with eight S-components, seven of which are non-homologous at the sequence level and shown or predicted to bind different substrates (chapter 3). In this way one ECF module

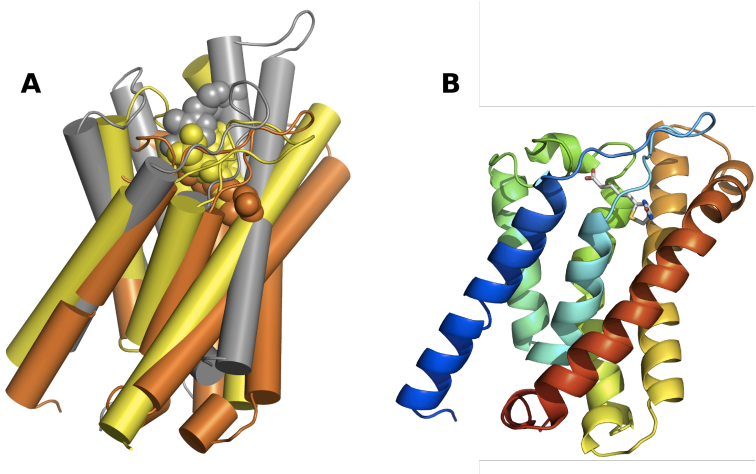

Figure 1.7. **Structures of S-components with substrate bound. A** RibU from *Staphylococcus aureus* (in yellow PDB: 3P5N), ThiT (PDB: 3RLB in grey) and BioY (in orange PDB: 4DVE) from *Lactococcus lactis* were aligned based on their structures. The substrates are shown as spheres and the binding sites are located at approximately the same location. **B** The structure of BioY (indicated as secondary structure cartoon in rainbow colors from blue at the N-terminus to red at the C-terminus) with biotin (shown as sticks) bound. The long L1-loop between the first helix as well as the C-terminal half (helices 4-6) are involved directly in ligand binding.

can form various EcfAA(')T-S-component complexes and these different complexes can transport various substrates (chapter 3).

The ECF module was already predicted in 1979 by Gary Henderson and colleagues (Henderson et al., 1979). They studied *Lactobacillus casei* and found that folate, biotin and thiamin bound to different integral membrane proteins (now known to be S-components). Although these vitamins did not compete with each other for binding, they did compete for transport, but only when their binding proteins were expressed. Henderson and colleagues concluded that, in addition to the distinct binding proteins, transport of these three substrates depended on a common component that was present in limited amounts. They speculated that this component might be a protein required for the coupling of energy to the transport process. This observation is consistent with the notion that S-components rely on the ECF module for transport and is where the name ECF, Energy Coupling Factor, comes from. Since competition depended on the presence of substrate the data also indicates that S-components with substrate bound have a higher affinity for the ECF module than when they are in the apo-state. Probably this difference in affinity is due to a change in conformation upon substrate binding, which (as stated above) is likely to involve the closure of the L1 loop.

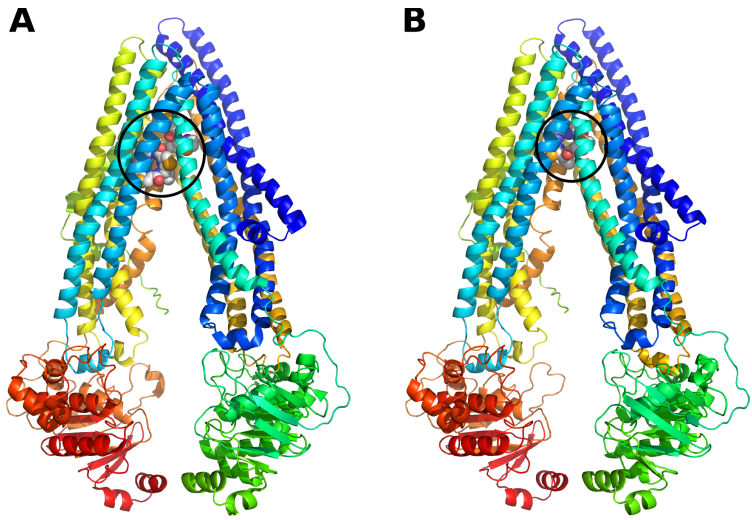

Figure 1.8. **P-glycoprotein (Pgp) with two QZ59-SSS molecules bound in the upper and lower binding site (A) or one QZ59-RRR bound in the middle binding site (B) in the internal cavity.** The cyclic inhibitors are rendered as spheres and for clarity a black circle is drawn to show where they are, while the Pgp is shown as a cartoon in rainbow colors from blue at the N-terminus till red at the C-terminus.

1.6.3 ABC exporters

Exporters also do not use a separate binding protein. Very few structural details are known about substrate binding in ABC exporters. P-glycoprotein (Pgp, also known as MDR1 or ABCB1) is known to transport hundreds of substrates ranging from 300 to 40000 Da (Ambudkar et al., 2003; Aller et al., 2009). Most of its substrate are hydrophobic and partition in the lipid bilayer. Two structures of Pgp from mouse (87% identity with the human homolog that is involved in multidrug resistance of cancer cells) with different cyclic inhibitors gave some information about the drug binding site (Aller et al., 2009). These inhibitors inhibit drug-stimulated ATPase activity and drug transport in a concentration dependent manner. The proposed drug-binding cavity of Pgp is large (6000 $Å^3$) and the two inhibitors were co-crystallized while they were bound at different positions (figure 1.8). Three binding sites (higher, middle and lower) for the inhibitors were identified within the cavity. Two portals were found ($\sim$9 diameter at the widest point) via which drugs or lipids could enter from the inner leaflet of the lipid bilayer or from the cytoplasm into the drug-binding cavity. The portals were formed by TM helices 4, 6, 10 and 12, that could hypothetically pack tightly in an outward conformation to close and prevent substrates to go back to the cytosollic-site during extrusion.

1.7 Translocation cycle

1.7.1 Type I ABC importers

The best studied type I importer is the maltose transporter $MalFGK_2$. This transporter will be described as the only example of type I transporters, but structures of other type I systems are available (table 1.1). There are crystal structures of $MalFGK_2$ in an outward facing catalytic intermediate state, an inward facing conformation and in a so-called pre-translocation intermediate state (figure 1.9) (Oldham et al., 2007; Khare et al., 2009; Oldham & Chen, 2011a). The outward facing conformation is a structure of a mutated transporter with ATP, but without Mg^{2+}. The other $MalFGK_2$ structures do not have any nucleotides bound.

In the outward facing catalytic intermediate the translocation pathway between the two TMDs of $MalFGK_2$ is open towards the maltose-binding protein (MBP, the SBP for maltose), which is bound to the transmembrane domains. The MBP is in a ligand-free open conformation and docked onto the two TMDs, from the periplasmic site. The two lobes of the MBP make extensive contacts with the TMDs and are in this way preventing maltose to diffuse back to the periplasm. Thus, the MBP imposes directionality on the transport process. One of the periplasmic loops of the TMD MalG inserts into the sugar-binding cleft of the MBP. This insertion possibly forces the two lobes of the substrate-binding protein open to release maltose into the translocation pore. Maltose is bound about halfway the membrane on the interface between the two TMDs: MalF and MalG. This binding site has an estimated K_d of 1 mM (Treptow & Shuman, 1985). Ten residues of MalF interact with the maltose molecule by stacking with the sugar rings, hydrogen bonding and van der Waals interactions. Interestingly no residues of the other TMD (MalG) interact with maltose.

In the inward facing conformation the core helices of the TMDs are maintained as rigid bodies with respect to the outward facing structure, but they are rotated 22° (core of MalF) and 23° (MalG core) and have a ∼4 Å translation along the rotational axes. The rotational axes of MalF and MalG are both at an angle of ∼45° to the membrane plane and are nearly orthogonal to each other. The NBDs are in an open conformation, as expected in the absence of nucleotide and are rotated 14° with respect to the closed conformation in the outward facing state (aligned by the additional C-terminal domain and with the rotational axis roughly perpendicular

to the plane of the membrane). The maltose-binding site in MalF is in this structure closed off from the periplasm by a hydrophobic gate and accessible from the inside of the cell. The hydrophobic gate is formed by four loops at the bend of kinked TM helices. A rigid body movement thus accomplishes the shift from outward to inward facing conformation without significant changes within the TMD subunits.

In the pre-translocation intermediate state (Oldham & Chen, 2011a) the maltose-binding protein is docked onto the TMDs, but in a closed state with the maltose still bound to the MBP. The periplasmic gate observed in the inward-facing structure is still intact, but the maltose-binding site of MalF is also closed off from the cytosol. The periplasmic gate is the same as in the inward-facing structure, but the cytosolic one is different from the outward-facing structure. In this structure there is not a bundle of helices closing off the cytosol, but only a few residues of the two TMDs that interact via van der Waals interactions. Because of the absence of ATP, the NBDs are in a semi-open conformation, although they are closer together than in the completely open state. The D-loops of the NBDs are interacting, but the domains are not yet rotated towards each other. This structure was interpreted as an intermediate between the inward-facing resting state conformation and the outward-facing conformation. Presumably the binding of the MBP makes the transporter go from an inward-facing conformation to this state, but ATP has to be bound to be able to switch the transporter further to a completely outward-facing state. When AMP-PNP (a nonhydrolyzable ATP analog) was added to the crystals of the wildtype proteins in this pre-translocation intermediate state, they indeed shifted to an outward-facing conformation. Other crystals were used in which the MBP was cross-linked in such a way that it could not open and in these crystals the shift of conformation upon AMP-PNP addition was not observed. This suggests that the three processes of ATP binding, shifting to the outside-facing conformation and opening of the MBP are linked. Subsequent analysis with electron paramagnetic resonance spectroscopy (EPR) strengthened this hypothesis (see below) (Orelle et al., 2010).

There are additional outward-facing conformation structures of the wildtype transporter with Mg^{2+} and AMP-PNP, ADP-BeF_3, ADP-VO_4 or ADP-AlF_4 bound (Oldham & Chen, 2011b). All these nucleotides resemble ATP or ADP + P_i. Since the ADP+P_i analogs could block the transporter in an outward-facing conformation, it seems that it is not the chemical reaction of the ATP hydrolysis that makes the transporter switch back to the inward-facing conformation, but rather the dissociation of ADP and P_i (Oldham & Chen, 2011b).

Besides structural data there is a large amount of additional biochemical data for type I transporters. In the intact maltose transporter ATP binding triggers high-affinity binding of the SBP to the extracellular regions of the TMDs (Chen et al., 2001). It has also been shown that the NBD dimer interface is not closed by ATP until the SBP is present, even though ATP is enough to close the NBDs when they are studied in isolation (Orelle et al., 2008). This observation explains how the SBP can stimulate ATPase activity (Davidson et al., 1992; Petronilli & Ames, 1991). Although ATP hydrolysis also occurs when SBP is added without substrate it is additionally increased in the presence of substrate (shown for the type I maltose transporter and histidine importer) (Davidson et al., 1992; Liu et al., 1997).

Other studies showed that the maltose-binding protein has a much higher affinity for the transporter when it is in a closed state (Millet et al., 2003), which is stabilized when maltose is bound. Site-directed spin labeling combined with electron paramagnetic resonance spectroscopy with labels on both lobes of the MBP showed that the SBP became tightly bound to the transporter in a vanadate-trapped transition state with both lobes completely immobilized and with a loss of spin-spin interaction, indicating an open conformation (Austermuhle et al., 2004). Binding of non-hydrolysable ATP analogs or ATP without Mg^{2+} was enough to stabilize the transporter-SBP complex with the SPB in an open conformation. This suggests that closure of the NBDs on one site of the membrane coincides with opening of the SBP at the opposite side of the membrane and release of the substrate from the SBP into the translocation channel (Austermuhle et al., 2004). After ATP is hydrolyzed, when MgADP and the SBP are still bound, the NBDs remain in a semi-open conformation. It is proposed that the transmembrane helices are reset to an inward-facing conformation during P_i release (Orelle et al., 2008).

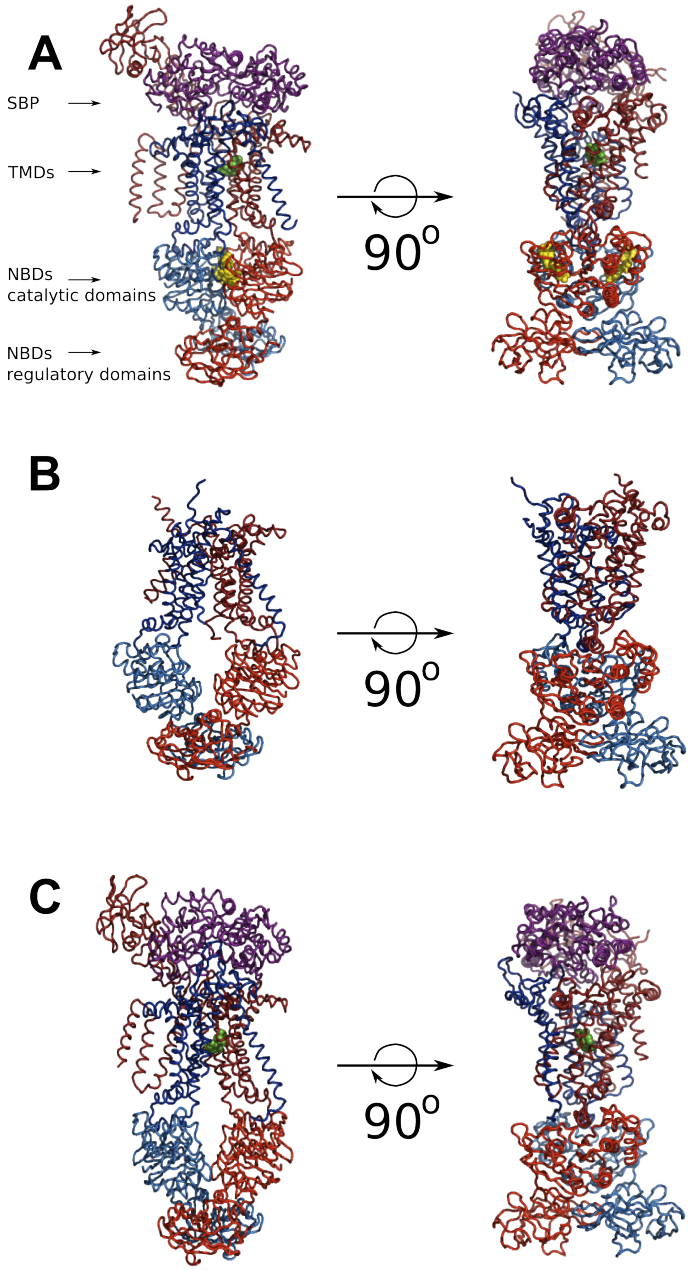

Figure 1.9. **Cartoon representation of the crystal structures of the type I maltose transporter (MalGFK$_2$ with and without the maltose-binding protein) from *Escherichia coli*.** MalG is colored dark blue, MalF dark red and of the two NBDs of MalK one is light blue and the other red, when present the maltose binding protein (MBP) is colored in purple. MalK contains a C-terminal regulatory domain, that is not present in all type I transporters. The (sub)domains are indicated with arrows in A. **A** Outward-facing catalytic intermediate state with MBP and two ATP bound. Maltose is present in the translocation channel bound to MalF. PDB code: 2R6G, resolution 2.8 Å. Maltose is shown in green and ATP in yellow spheres. **B** Resting state (inward facing conformation) without MBP or nucleotides. PDB code: 3FH6, resolution 4.5 Å. **C** Pre-translocation state with MBP and maltose (shown in green spheres) bound, but without nucleotides. PDB code: 3PV0, resolution 3.1 Å

1.7.2 Type II ABC importers

Structures of the vitamin B_{12} transporters $BtuC_2D_2$ with and without its substrate-binding protein BtuF (Hvorup et al., 2007; Locher et al., 2002) and the homologous $Hi1470_2/1471_2$ (=$MolB_2C_2$) protein without its SBP Hi1472 (=MolA) (Pinkett et al., 2007) have been determined. The two transporters have 24 and 33% identity between the TMD and the NBD subunits, respectively. The TM helices 3, 4, 5 and 5a can adopt two different conformations, resulting in an outward (crystal structure of $BtuC_2D_2$) and an inward (crystal structure of $Hi1470_2/1471_2$) conformation of the transporter or an occluded translocation pathway (crystal structure of $BtuC_2D_2F$) with one subset of TMs in one conformation and the other subset in the second conformation (figure 1.10 and 1.11).

In the outward structure of $BtuC_2D_2$ (Locher et al., 2002), the two copies of BtuC pack with their TM helix 5 against the TM helix 10 of the other subunit at a crossing angle of -143°, over a total surface area of 1800 $Å^2$. The cavity that is present in between these four helices is open from the outside and penetrates around two-thirds of the membrane. This cavity is sufficiently large to fit in most of a vitamin B_{12} (cobalamin, structure shown in table 1.2) molecule (although further conformational changes would be needed to fit the whole molecule) and is expected to be the translocation pathway. This translocation pathway is lined by hydrophobic residues from helices 5, 5a and 10 and by the non helical loops preceding TM helix 3 and 8. The cavity is closed off from the cytoplasm by Thr 142 and Ser 143 that are located in the loop between TM helix 4 and 5. The residues lining the periplasmic site of the cavity were only partly resolved, possibly because the SBP is absent.

When this outward facing structure is compared with the inward facing structure of $Hi1470_2/1471_2$ (=$MolB_2C_2$) by aligning one of the two TMDs, the other TMD is rotated ∼9°. When single TMDs are aligned around the central TM helix 2, most other TM helices also align very well except for helices 3, 4 and 5. Helix 5 is rotated by 20° around the central helix 2 and since helix 5 is located at the dimer interface, the result is a rotation between the two TMDs. The TM helices 5 and 10 from two Hi1471 subunits in the inward facing conformation cross at -163° instead of -143° (found in the outward facing structure of $BtuC_2D_2$) (Pinkett et al., 2007). These rearrangements open up the translocation pore at the cytoplasmic site, while at the same time closing the opening towards the periplasmic site that was present in the $BtuC_2D_2$ structure. The extramembrane helix 5a that directly follows TM helix 5 plays an important role in closing off the access to the periplasm.

None of the type II importer structures have nucleotides bound in the NBDs. The NBD dimer of $BtuD_2$ in the $BtuC_2D_2$ structure and the Hi1470 dimer mostly resemble the semi-open NBD state found for $MalK_2$ with ADP bound (Chen et al., 2003), although the Hi1470 dimer without nucleotides bound is slightly more open than BtuD2, which had cyclo-tetra-vanadate bound in the ATP binding site (Pinkett et al., 2007). Cyclo-tetra-vanadate $(VO_3)^4$ is the prevalent species of ortho-vanadate at the pH that was used for crystal growth. Monomeric vanadate is used as a P_i mimic and blocks ABC transporters in the ADP+P_i state. In the structure cyclotetravanadate is bound at the location of the α- and β-phosphate of ATP/ADP (Pinkett et al., 2007). When one NBD of the Hi1470 dimer is aligned to one of the BtuDs, the none-aligned NBDs are shifted by a translation of $\sim$4.5 Å along an axis parallel to the NBD interface. This motion occurs at the same time as the rotation direction of the TMDs. Also taking the structural data of type I importers and exporters into account, this suggest that $BtuC_2D_2$ represents the ATP-bound outward-facing conformation, even though it has no ATP bound (Pinkett et al., 2007).

There is also a crystal structure of $BtuC_2D_2$ with its substrate binding protein BtuF, but without the cyclovanadate (Hvorup et al., 2007). This crystal structure, that is closed from both sides and has a translocation pore that is probably not large enough for vitamin B_{12}, was hypothesized to be a posttranslocation intermediate. In this structure BtuF has no vitamin B_{12} bound and is in an open conformation interacting with both BtuC subunits. When BtuF was crystallized in isolation there was very little difference found in its conformation with or without substrate; in both cases it was crystallized in a closed conformation. However in the structure of the whole ABC transporter complex BtuF is in an open conformation with its lobes 4 Å shifted outward compared to the closed structures (figure 1.6). Each lobe of BtuF interacts mostly with one of the two BtuC subunits. Since the BtuF lobes are asymmetric, the periplasmic loops of $BtuC_2$ also are no longer completely symmetrical. Extensive interactions, amongst others salt bridges between conserved arginines from BtuC and glutamates from BtuF, link BtuF to the BtuC dimer. The periplasmic loop between TM helix 5 and extramembrane helix 5a from both BtuC subunits enter into the B_{12} binding site of BtuF, thereby preventing the substrate to bind. Probably this insertion displaces the bound vitamin from the SBP. As in the outward facing structure without the SBP the NBDs ($BtuD_2$) are in a semi-open conformation, with the P-loop and the ABC signature motif apart from each other. While there was a clear two-fold symmetry in the $BtuC_2D_2$ structure, the

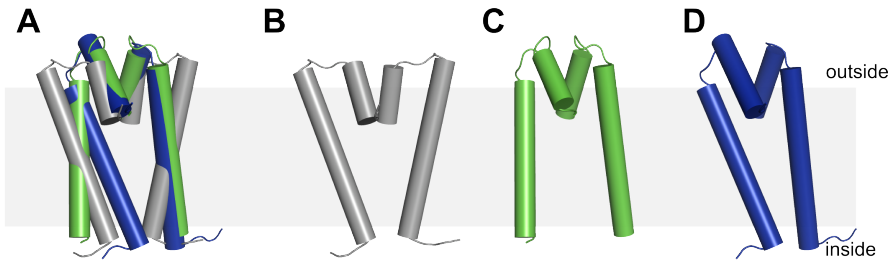

Figure 1.10. **Cartoon representation of TM helix 5 and the short helix 5a of both TMDs in the crystal structures of type II ABC importers. A** Overlay of the helixes from the different structures (the complete transporters were used for the alignment). **B** Outward-facing conformation of $BtuC_2D_2$, PDB code: 1L7V. **C** Inward facing conformation of $Hi1470_2/1471_2$, PDB code: 2NQ2. Both of the TM helices are rotated by 20° around the central helix 2, which results in an inward facing conformation. **D** Post-translocation state of $BtuC_2D_2$-BtuF, PDB code: 2QI9. One TM helix 5 is in the outward-facing conformation (the one depicted on the left), while the other one (here on the right) is in the inward-facing conformation. This leads to an occluded state.

BtuC subunits in the structure with BtuF are much more asymmetric, especially on the cytoplasmic site and in TM helices 3-5 and helix 5a. The subset of helices 3-5a seems to determine to which site of the membrane the translocation pore is opened (figure 1.10). The helices 3-5a of the BtuC subunit that interacts mostly with the C-terminal lobe of BtuF are in a similar conformation as in the outward facing structure without BtuF, while the other set of TM helices 3-5a that mostly interacts with the N-terminal lobe, are in a similar conformation as the inward-facing $Hi1470_2/1471_2$ structure. There are hydrophobic residues in TM helix 5 and helix 5a that close the central pore off from the cytoplasm and from the periplasm. Analogous hydrophobic residues are also found in other type II transporters and they are probably involved in the gating.

In summary, in type II ABC importers the transition from an inward to an outward facing conformation is primarily accomplished by a change in the tilt of TM helix 5 that lines the translocation pore (figure 1.10). The structures of type II transporters suggest a mechanism, in which a translational shift of the NBDs along the dimer interface is coupled to a twisting motion in the TMDs that turns them from an inward to an outward facing conformation or *vice versa* (Jones et al., 2009). The NBDs of type II ABC importers therefore move in a perpendicular direction compared to the NBDs of type I importers and exporters such that they remain in contact during the translocation cycle. This distinct mechanism for type II importers was further supported by electron spin resonance studies based on the crystal structures (Goetz et al., 2009; Joseph et al., 2011) . These studies also suggested that unlike the type I importer and exporter types, type II importers

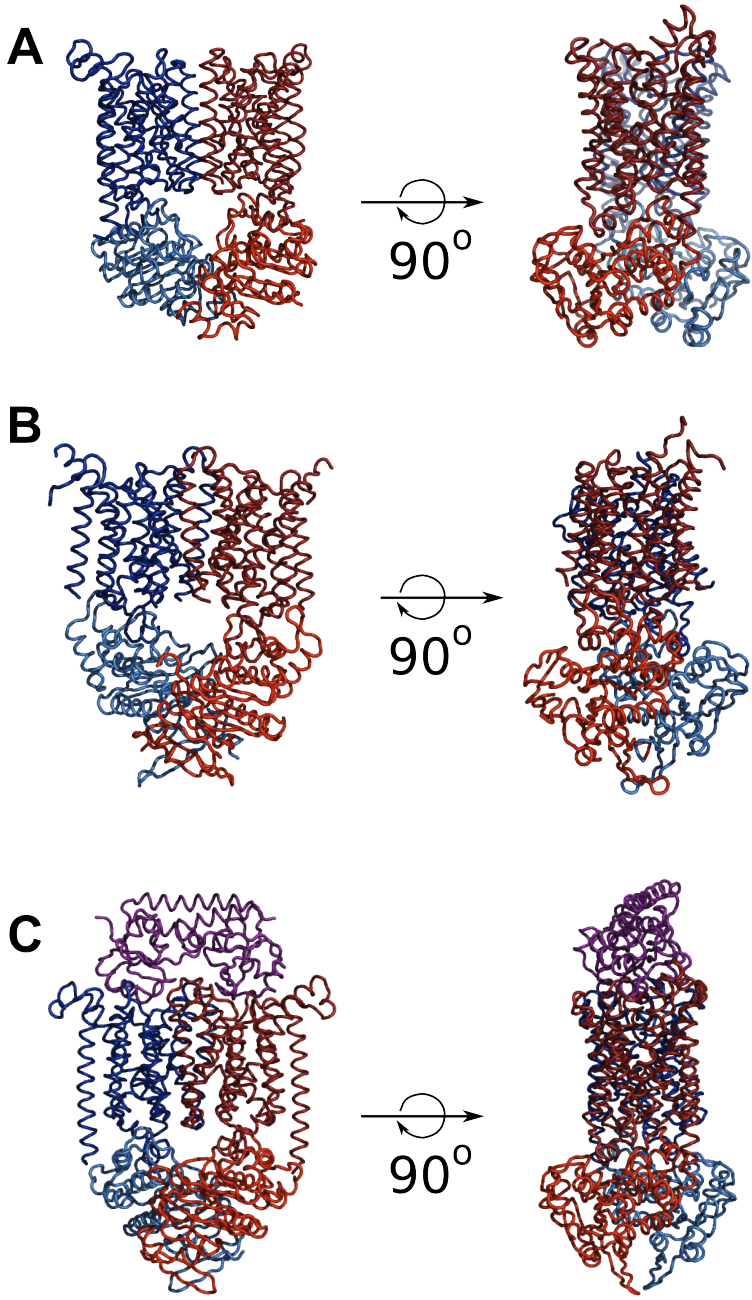

Figure 1.11. **Cartoon representation of the crystal structures of type II ABC importers.** The TMDs are colored dark blue and dark red, the NBDs are light blue and red, and when present the SBP is colored in purple. **A** Outward facing conformation of $BtuC_2D_2$, PDB code: 1L7V, resolution 3.2 Å. **B** Inward facing conformation of $Hi1470_2/1471_2$, PDB code: 2NQ2, resolution 2.4 Å. **C** Post-translocation state of $BtuC_2D_2$ complexed with its SBP: BtuF. PDB code: 2QI9, resolution 2.6 Å.

would open to the cytoplasmic side for substrate release when ATP was bound, although another study on a homologous heme transporter found that not ATP binding but ATP hydrolysis triggered release of the substrate on the cytoplasmic site (Burkhard & Wilks, 2008).

For the maltose ($MalFGK_2$) and other ABC type I importers it has been shown that the SBPs have a low affinity for the TMDs of the transporter (K_d of $\sim 10^{-4}$ M) and only interact with the transporter transiently (Lewinson et al., 2010; Merino et al., 1995; Ames et al., 1996; Doeven et al., 2004). However, for two type II transporters it was shown that their SBPs (BtuF and Hi1472=MolA) bind with high affinity to the periplasmic site of the TMDs and form stable complexes. The $BtuC_2D_2$-BtuF complex has a K_d of $\sim 10^{-13}$ M and the $Hi1470_2/1471_2$-Hi1472 ($MolB_2C_2$-A) complex has a K_d of 10^{-9} M (Lewinson et al., 2010). The difference in affinity in type I or type II importers, probably explains why the $BtuC_2D_2$-BtuF complex could be crystallized in the absence of nucleotides, while for type I importers a non-hydrolysable ATP analog is needed to get a complex with the SBP. In fact the $BtuC_2D_2$-BtuF complex was destabilized by the presence of substrate and ATP. The SBP, BtuF, only gives a two-fold increase in the ATP hydrolysis activity of $BtuC_2D_2$ and this increase is independent of whether BtuF has substrate bound or not. In the type I maltose and histidine transporters, there is a much larger increase in ATP hydrolysis but only with substrate loaded SBP. It is not yet known how substrate translocation and ATP hydrolysis are coupled in type II transporters, but the difference in the movement between inward-facing and outward-facing conformation and the differences in SBP binding compared to type I transporters show that there is a considerable mechanistic diversity within ABC importers.

The crystallized type I transporters contain cluster D SBPs that contain flexible loops in the hinge region between the two domains (table 1.3). These are the MBP of $MalFGK_2$ from *E. coli*, ModA of $ModB_2C_2$ from both *A. fulgidus* and *M. acetivorans*. For the third crystallized type I transporter MetNI the SBP has not been crystalized. To date all identified type II importers have cluster A substrate-binding protein. These are BtuF of $BtuC_2D_2$ and Hi1472 (MolA) of $Hi1470_2/1471_2$ ($MolB_2C_2$). The recently crystallized MolA or Hi1472 is the first cluster A SBP for molybdate/tungstate, while the two crystallized type I importers for molybdate/tungstate have cluster D SBPs (Tirado-Lee et al., 2011) (table 1.3, cluster D3, tetrahedral oxyanions (Berntsson et al., 2010)). The distinguishing feature of cluster A SBPs is the α-helix that forms the hinge region (table 1.3) (Berntsson et al., 2010). This helix makes the structure of these SBP rather rigid

and only small domain movements in domain opening and closing have been reported (figure 1.6). Structural alignment of MolA with two other crystallized cluster A SBPs with very different substrate specificities, namely BtuF (much larger substrate: vitamin B_{12}) and TroA (smaller substrate: zinc), showed that they have a very similar fold (rmsd of 3.2 and 3.5 Å respectively) even though there is very little sequence identity (respectively 18 and 9 % identity) (Tirado-Lee et al., 2011). Not surprisingly, the largest variations are in the loops that determine the size of the substrate-binding pocket. Because of the small conformational change reported for cluster A SPBs, not only the binding pocket itself, but also the accessibility towards it, was suggested to add to the selectivity of substrate binding (Tirado-Lee et al., 2011). It was also shown that MolA has a lower affinity for its substrate than other molybdate/tungstate binding proteins that interact with type I transporters (Tirado-Lee et al., 2011), whether this is a general feature of cluster A SBPs will need further investigation.

The small conformational changes between substrate-bound and unliganded SBP, might also explain the high affinity that was found in case of BtuF and Hi1472=MolA for the rest of the transporter in absence of substrate. This might thus be a difference between cluster A and other SBPs instead of between type I and type II transporters. On the other hand it is also possible that all type II transporters have cluster A substrate-binding proteins.

1.7.3 Type III or ECF-type importers

So far, no EcfAA(')T-S-component complex has been crystallized and much less is known about the mechanism of this type of transporter. There are crystal structures available from EcfA proteins (PDB: 3GFO, 2PJZ, 2YZ2), which show the typical NBD fold (figure 1.4) and all EcfA and EcfA' proteins contain all the conserved sequence motifs (figure 1.3). There are also structures available from three different S-components (discussed earlier under substrate binding). The dynamic interaction between the S-component and the ECF module seems to be an important part of the functional mechanism of ECF transporters (chaper 5). What we know about the functional mechanism of the ECF-type transporters is based on biochemical data and the S-component structures.

The lack of structural information and varying results from biochemical data on different ECF-transporters has led to two different hypothesis for the oligomeric state of the complexes and two different mechanistic models. Figure 1.12 shows

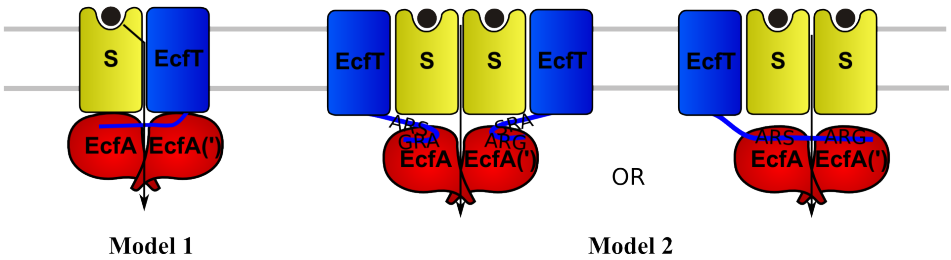

Figure 1.12. **Translocation model 1 and 2 for ECF-type ABC transporters differ in the stoichiometry of the different proteins of the EcfAA(')T-S-component complex and the location of the translocation pathway (indicated with a black arrow).**

the largest differences of the two proposed models in a cartoon. Both models will be discussed below.

Model 1

This model is based on the 1:1:1:1 stoichiometry (EcfA:EcfA':EcfT:S-component) that was found for detergent-solubilized and purified EcfAA'T-S-component complexes from *L. lactis* (determined by size-exclusion chromatography coupled to multi-angle laser light-scattering (SEC-MALLS) analysis, chapter 3). This stoichiometry is also suggested by the presence of gene fusions in some organisms. Sometimes only one EcfA component is encoded in the operon of the ECF module, but two EcfA components (EcfAA') are more common and in several cases the two are fused. There are two genomes where the S-component is fused to two EcfA domains, in four cases EcfT is fused to two EcfA domains and there is one fusion of an S-component with an EcfT (chapter 2) (D. Rodionov et al., 2009).

The other biochemical data that was taken into account is that (most) S-components do not support transport without the ECF module (chapter 2, 4, 5 and (Zhang et al., 2010; Erkens et al., 2011; D. Rodionov et al., 2009; Eudes et al., 2008; Neubauer et al., 2009)). The structural data that was used is based on the S-component structures of RibU (from *Staphylococcus aureus*) (Zhang et al., 2010), ThiT (from *Lactococcus lactis*) (Erkens et al., 2011) and the structure of BioY (also from *Lactococcus lactis*, chapter 4). The analysis of this data will now be discussed.

S-components are predicted to interact with an EcfAA(')T complex. This interaction has been experimentally confirmed for all crystallized S-components. Since S-components are very hydrophobic and contain only small extracellular/cytoplasmic

loops, interaction is expected to take place to a large extend via interaction of TM segments of S-components with TM segments from EcfT. *L. lactis* contains a homologue of the RibU that was crystallized and this protein interacts with the same EcfT as the crystallized ThiT and BioY. When BioY, ThiT and RibU were aligned helices 1-3 (the N-terminal domain) align much better than helices 4-6 (the C-terminal domain, figure 1.13, chapter 4 and (Erkens et al., 2011)). Presumably the N-terminal domain is conserved to interact with the EcfT, while the C-terminal domain differs to accommodate the high-affinity binding of the different substrates. Interestingly, the BioY structure was less similar to ThiT than to RibU from *S. aureus*, while BioY and ThiT come from the same organism (*L. lactis*) and have to interact with the exact same EcfT.

In the S-components from *Lactococcus lactis* the only conserved residues were two alanines spaced by three residues (Erkens et al., 2011). In the crystal structure the alanine residues are at the lipid-exposed protein surface of helix 1. AxxxA or GxxxG motifs (with x any amino acid, mostly hydrophobic) are known to promote helix packing in the lipid bilayer. When one of these alanines was mutated into a bulky tryptophan the binding of thiamin to isolated ThiT was not affected but thiamin transport was abolished. Mutated ThiT was also no longer copurified with the ECF module (Erkens et al., 2011) while wildtype ThiT did copurify (chapter 3), strongly indicating that indeed these alanines in ThiT are important for the interaction with the EcfAA'T.

A possible model for translocation is shown in figure 1.12 (based on chapter 3, 4, 7 and (Erkens et al., 2011)). In this model rearrangements of the L1 loop would perturb the binding site and at the same time open a lateral gate towards the predicted interface between the two TMDs (the S-component and EcfT). The substrate would then be transported over the membrane through a translocation channel in between the two transmembrane domains, as is the case in all other types of ABC transporters. The translocation cycle and structural rearrangements must be driven by ATP hydrolysis in the ATPase domains. The structural rearrangements in these domains have to be transferred to the S-component. A cytosolic helix that could couple the S-component to one of the NBDs was not found in any of the structures. Such coupling helices were observed in the TMDs of all other ABC transporters of which the structure is known. Possibly the coupling between the ATP hydrolysis in the NBDs and substrate release and translocation via the TMDs, is solely mediated via EcfT, which might have two coupling helices (Erkens et al., 2011).

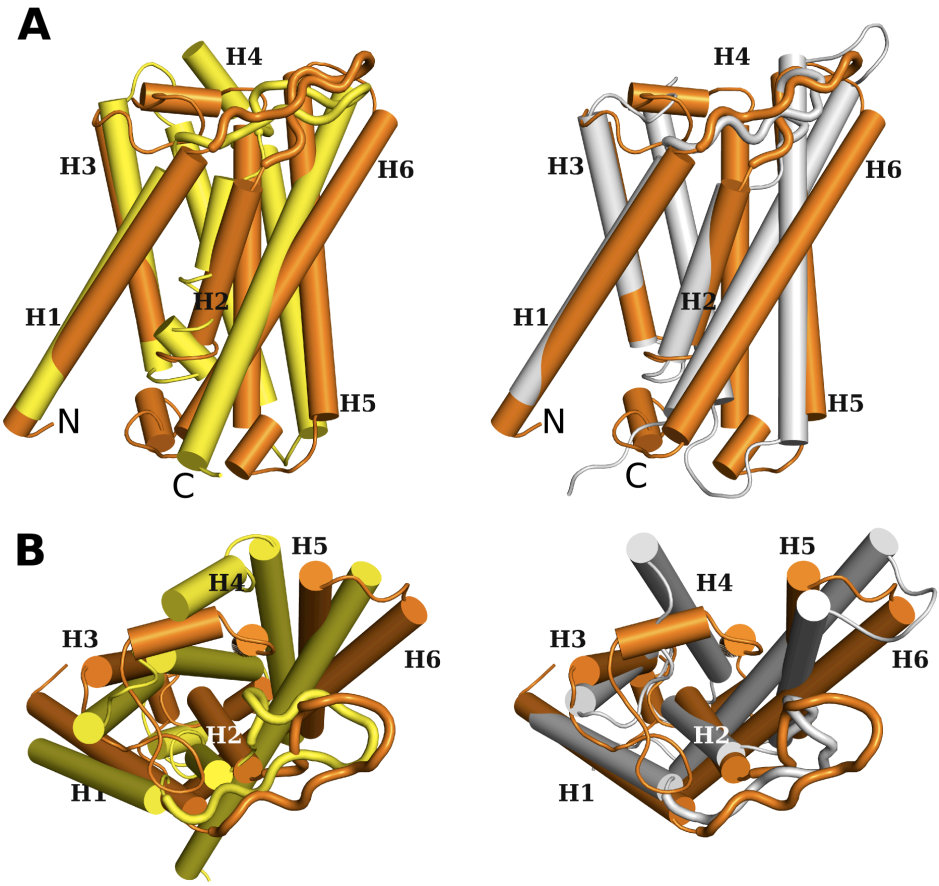

Figure 1.13. **The three available structures of S-components with substrate bound aligned via TM helices 1-3.** Superimposed structures of BioY from *Lactococcus lactis* (PDB: 4DVE, chapter 4) in orange, with RibU from *Staphylococcus aureus* (PDB: 3P5N) in yellow, or ThiT (PDB: 3RLB) from *Lactococcus lactis* in grey. The structures are viewed from the plane of the membrane (panel A) and from the outside of the cell (panel B, direction of view perpendicular to the membrane plane). The structures have been superimposed on helices 1 & 3 in order to highlight the structural similarities of helices 1-3 and the differences of helices 4-6. Loops 1 are indicated in thick lines. The N- and C-terminus are marked with N and C, respectively (panel A). Helices 1-6 are marked with H1-H6.

We hypothesize that ECF transporters are more likely to resemble type II importers than type I importers or ABC exporters. The reason for this is that it will be unlikely that the TMDs of EcfT and the S-component will intertwine, since in the absence of the EcfT the S-components fold into stable membrane proteins that bind substrate (Duurkens et al., 2007; Erkens & Slotboom, 2010; Eudes et al., 2008; Vogl et al., 2007) and because an S-component that is bound to the EcfAA(')T complex can exchange for another one (chapter 5). The transport via EcfAA(')T-S-component complexes will probably go via a teflon-like surface, without an additional substrate-binding

site halfway the membrane as was observed for the type I transporter $MalFGK_2$. This is because the substrates that are transported by one and the same EcfAA(')T can vary so widely (see table 1.2 for a list of all the ECF substrates and table 3.1 for a list of the substrates of the general EcfAA'T from *L. lactis*). It will thus be unlikely that the EcfT will have a binding site for all these substrates. It is also unlikely that this additional binding site in the translocation pore will be formed by the S-component alone, since no obvious translocation pathway or additional binding site was found for any studied S-component besides the main high-affinity binding site at the periplasmic site of the membrane (chapter 4 and (Duurkens et al., 2007; Erkens & Slotboom, 2010; Eudes et al., 2008; Vogl et al., 2007)).

Model 2

This model is based on studies on BioY and BioMNY from *R. capsulatus*, (Neubauer et al., 2011, 2009; Finkenwirth et al., 2010; Hebbeln et al., 2007). The model mostly differs because of the experimental findings that BioY can catalyze transport without the ECF module (Hebbeln et al., 2007) and that BioY forms oligomers in the membrane (Finkenwirth et al., 2010). Since BioY was reported to be an oligomer and to support transport without the BioMN, two copies of the S-component (a BioY homodimer) were predicted to line the translocation pore (figure 1.12) (Finkenwirth et al., 2010). In the BioMNY complex these BioY dimers are predicted to be associated with one or two copies of BioN (EcfT). The ATPase dimer is formed by two copies of the same EcfA (BioM) (Finkenwirth et al., 2010; Neubauer et al., 2011). For a discussion of the different experimental observations see chapter 7.

In EcfT a conserved ARS-ARG motif was found that was predicted to be present in a long cytosolic loop. It was shown to be important for EcfA-EcfT (BioM-BioN) interactions (Neubauer et al., 2009, 2011). When residues in and around the ARS-ARG motif were mutated into cysteines they could be crosslinked to engineered cysteines around the Q-loop in the ATPase BioN. This part of model 2 can also be incorporated in model 1, where the interaction with the EcfA(') domains is also expected to be largely accommodated by EcfT, since no coupling helix could be found in the S-component.

1.7.4 ABC exporters

Based on biochemical experiments ATP binding is expected to shift exporters from an inward facing conformation (where it is expected to bind its substrate), to an outward facing conformation. How this movement occurs can be hypothesized based on the crystal structures of MsbA (a lipid flippase, figure 1.14). The difference between the inward and the outward facing structure has been described as two motions, although probably they occur simulataneously in the translocation cycle (Ward et al., 2007). The first motion is a 10° rotation around the extracellular loops between TM helices 3 and 4, and between helices 5 and 6. This movement brings the NBDs closer together. In the second motion the NBDs dimerize and form the site for ATP hydrolysis. Because of the closure of the NBDs, TM helix 4 and 5 are tilted by 20°. Since these two helices are connected to TM helix 3 and 6 via the extracellular loops mentioned in the first motion, the NBD dimerization pulls TM helices 3 and 6 away from helices 1 and 2. Together these two movements would change the inward-facing conformation to the outward-facing conformation that was found in the open crystal structure. On the basis of the static crystal structures it can thus be explained or at least hypothesized how the change in conformation of the NBDs, triggered by binding and hydrolysis of ATP and release of ADP and P_i, brings about the large rearrangements in the TMDs.

The alternating access model implies that the inward facing conformation is likely to have a higher affinity for substrate binding from the inner leaflet of the membrane or from the cytosol than the outward conformation. The latter would allow the substrate to be released in the external medium (or outer leaflet of the membrane). The inward opening of ABC exporters is formed by TM helices 3/6 and 4/5, while the outward opening is formed by helices 3/6 and 1/2. Since both conformations thus have different TM helices that line the cavity, differences in binding affinity are indeed likely. In the drug-exporter LmrA from *L. lactis* two drug binding sites with different affinities were indeed found and when LmrA was blocked by ADP with vanadate only the low affinity binding site was accessible (Veen et al., 2000).

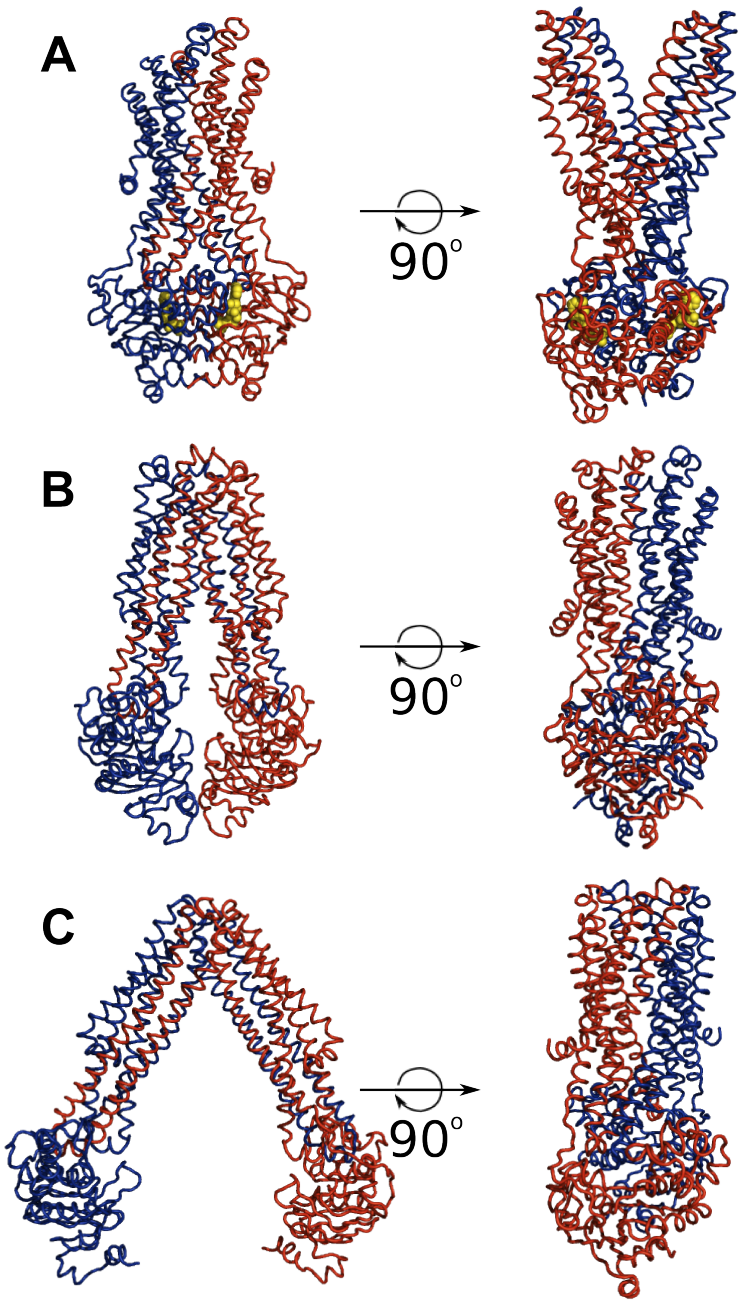

Figure 1.14. **Crystal structures of the ABC exporter and lipid flippase MsbA in three different states.** The two polypeptide chains are shown in red and blue. **A** Structure of MsbA from *Salmonella typhimurium*, open towards the outside with ANP-PNP bound (shown in yellow spheres). PDB code: 3B60, resolution 3.7 Å. **B** Structure of MsbA from *Vibrio cholerae*, no nucleotides bound. PDB code: 3B5X, resolution 5.5 Å. **C** Structure of MsbA from *E. coli*, no nucleotides bound. PDB code: 3B5W, resolution 5.3 Å.

1.7.5 Concluding remarks

The mechanisms of ABC transporters described so far vary widely. In type I ABC importers there is a rigid-body motion in the TMDs during translocation, in type II importers the change from an inward to outward facing structure is obtained by subtle intersubunit changes, while in exporters there is a radical rearrangement of the TM helices. It will be important to determine the mechanism of translocation by ECF-type importers, which may yield another mechanism of transport.

1.8 Outline of this thesis

The rest of this thesis describes the ECF-type ABC importers. **Chapter 2** describes the discovery of this type of transporters.

In **chapter 3** the ECF module from *Lactococcus lactis* is described that was predicted to interact with eight different S-components. The ECF module was co-expressed with all S-components, one at the time, in *E. coli* cells. We showed that indeed all eight different EcfAA'T-S-component complexes can be formed and purified. With the use of size-exclusion chromatography coupled to multi-angle laser light scattering (SEC-MALLS) we showed that the purified EcfAA'T-S-component complexes consist of a single copy of each of the four proteins. Two of these complexes were functionally reconstituted in proteoliposomes, and were shown to transport their substrates in an ATP-dependent manner.

Chapter 4 is dedicated to the S-component for biotin, BioY, from *L. lactis*. The crystal structure was determined at high resolution and compared to the structures of RibU (the S-component for riboflavin) from *S. aureus* and ThiT (the S-component for thiamin) also from *L. lactis*. The overall fold is the same, but there are large variations, especially in the C-terminal domain (helix 4-6). We predict that this domain deviates to form the high affinity binding sites for the different substrates, while the N-terminal domain (helix 1-3) is more conserved to form the interaction site with the ECF module. BioY was found to have a high affinity for biotin (K_d 0.3 nM). When BioY was reconstituted in absence of the ECF module there was only biotin binding to proteoliposomes, but when EcfAA'T-BioY complexes were reconstituted ATP dependent biotin uptake could be measured.

Via recombinant protein expression in *E. coli* cells we show in **chapter 5** that the S-components for thiamin (ThiT) and for niacin (NiaX) are dependent on the ECF module to sustain transport. We also show that when ThiT, NiaX and the ECF module are co-expressed, the S-components can compete with each other for transport via the ECF module and that the competition depends on the substrate concentration. This data is consistent with the data from *Lactobacillus casei* cells by Henderson and colleagues in 1979 (Henderson et al., 1979) and shows that S-components have a higher affinity for the ECF module when they have substrate bound.

In **chapter 6** an effort is made to further characterize the EcfAA'T-S-component complexes. In this chapter substrate binding, complex stability and ATPase activity is described.

Chapter 7 gives a summary of the contents of this thesis, discusses the controversies about the structure and function of ECF-type transporters and proposes a model for substrate transport by ECF transporters.